Microbial colonizers of microplastics in an Arctic freshwater lake

Microbial colonizers of microplastics in an Arctic freshwater lake

Miguel González-Pleiter[1,†], David Velázquez[1,†], María Cristina Casero[2], Bjorn Tytgat[3], Elie Verleyen[3], Francisco Leganés[1], Roberto Rosal[4], Antonio Quesada[1], Francisca Fernández-Piñas[1,*]

[1] Departamento de Biología, Universidad Autónoma de Madrid, Cantoblanco, E-28049 Madrid, Spain

[2] Departamento de Biogeoquímica y Ecología Microbiana, Museo Nacional de Ciencias Naturales, CSIC, E-28006 Madrid, Spain

[3] Laboratory of Protistology & Aquatic Ecology, Ghent University, Krijgslaan 281-S8, 9000 Gent, Belgium

[4] Department of Chemical Engineering, University of Alcalá, E-28871 Alcalá de Henares, Madrid, Spain

[*] Corresponding author: francisca.pina@uam.es

[†] These authors contributed equally to this work.

Abstract

Microplastics (MPs) have been found everywhere as they are easily transported between environmental compartments. Through their transport, MPs are quickly colonized by microorganisms; this microbial community is known as the plastisphere. Here, we characterized the plastisphere of three MPs, one biodegradable (PHB) and two non-biodegradables (HDPE and LDPE), deployed in an Arctic freshwater lake for eleven days. The plastisphere was found to be complex, confirming that about a third of microbial colonizers were viable. Plastisphere was compared to microbial communities on the surrounding water and microbial mats on rocks at the bottom of the lake. Microbial mats followed by MPs showed the highest diversity regarding both prokaryotes and eukaryotes as compared to water samples; however, for fungi, MPs showed the highest diversity of the tested substrates. Significant differences on microbial assemblages on the three tested substrates were found; regarding microbial assemblages on MPs, bacterial genera found in polar environments such as *Mycoplana*, *Erythromicrobium* and *Rhodoferax* with species able to metabolize recalcitrant chemicals were abundant. Eukaryotic communities on MPs were characterized by the presence of ciliates of the genera *Stentor*, *Vorticella* and *Uroleptus* and the algae *Cryptomonas*, *Chlamydomonas*, *Tetraselmi*s and *Epipyxis*. These ciliates normally feed on algae so that the complexity of these assemblages may serve to unravel trophic relationships between co-existing taxa. Regarding fungal communities on MPs, the most abundant genera were *Betamyces*, *Cryptococcus*, *Arrhenia* and *Paranamyces*. MPs, particularly HDPE, were enriched in the *sulI* and *ermB* antibiotic resistance genes (ARGs) which may raise concerns about human health–related issues as ARGs may be transferred horizontally between bacteria. This study highlights the importance of proper waste management and clean-up protocols to protect the environmental health of pristine environments such as polar regions in a context of global dissemination of MPs which may co-transport microorganisms, some of them including ARGs.

Keywords: Microplastics; Arctic freshwater lake; Plastisphere; Microbial assemblages; Antibiotic resistance genes

1. Introduction

Plastic pollution is a cause of global concern. Anthropogenic activities annually produce millions of tons of plastics and an enormous amount of them ends up as debris in ecosystems every year. Once plastics reach the ecosystems, they are susceptible to degradation processes resulting in microplastics (plastic particles smaller than 5 mm; MPs), which may reach even remote regions (Ding et al., 2021; González-Pleiter et al., 2021; González-Pleiter et al., 2020a). In this context, the presence of MPs has already been well-documented in the Arctic environment: sediments (Bergmann et al., 2017; La Daana et al., 2020; Tekman et al., 2020; Woodall et al., 2014), sub-surface seawater (La Daana et al., 2018), seawater (Cincinelli et al., 2017; Cózar et al., 2017; Granberg et al., 2019; Huntington et al., 2020; La Daana et al., 2020; Lusher et al., 2015; Morgana et al., 2018; Rist et al., 2020;

Tekman et al., 2020), sea ice (Barrows et al., 2018; La Daana et al., 2020; Obbard et al., 2014; Peeken et al., 2018), snow (Bergmann et al., 2019), polar cod (Kühn et al., 2018), benthic organisms (Fang et al., 2021; Fang et al., 2018), amphipods (Imran et al., 2019), and seabirds (Amélineau et al., 2016; Bourdages et al., 2021; Poon et al., 2017). Just recently, data on MPs occurrence in Arctic freshwaters, one of the most important environments of this region, has been reported (González-Pleiter et al., 2020b). Freshwater bodies mostly consist of shallow permafrost lakes and ponds that contribute to the sustainment of the biodiversity of this ecosystem where microbial communities are the main components of the trophic webs with relevant roles in sustaining ecosystem structure and function as well as key players in mediating the biogeochemical cycling of nutrients (Garcia-Lopez et al., 2019; Perini et al., 2019; Sułowicz

et al., 2020). MPs may potentially impact composition, structure and diversity of microbial communities, altering for example microbiota composition and alpha diversity in soils and water (Agathokleous et al., 2021; Fei et al., 2020; Ma et al., 2020; Redondo-Hasselerharm et al., 2020; Wang et al., 2020a; Wright et al., 2021; Zhao et al., 2020). Alterations of these microbial communities may change the ecological balance and lead to severe effects for the Arctic biota (Walseng et al., 2018).

Due to their small size and recalcitrant nature, MPs are easily transported between environmental compartments. Thus, they constitute a durable and mobilizable substrate, which may be colonized by a range of microorganisms including bacteria, archaea, fungi, and protists. These colonizers conform the new biotope denoted as *plastisphere* (Amaral-Zettler et al., 2020; Zettler et al., 2013). Most reports about *plastisphere* derive from marine environments and only a few have targeted freshwater environments (Amaral-Zettler et al., 2020; Hoellein et al., 2014; Martínez-Campos et al., 2021; McCormick et al., 2016). Interestingly and as Amaral-Zettler et al., (2020) underpinned, most studies have been carried out in Europe, with only a few reports from Asia and America, and data lacking from Africa, polar regions or the Southern Hemisphere. Regarding the Arctic, apparently, there is a single report on the plastisphere of Arctic soils (Rüthi et al., 2020).

There is a growing concern that MPs might host pathogens of humans, fish, and corals, which due to the buoyancy and durability of the MPs may be transported greater distances; this may have severe ecological impacts as potential trophic transfer of these pathogens may occur due to potential ingestion, egestion and feeding on MPs by a number of organisms (Agathokleous et al., 2021; Amaral-Zettler et al., 2020; Imran et al., 2019; Kirstein et al., 2016; Lamb et al., 2018; Viršek et al., 2017). In addition, within attached microorganisms, there might be antibiotic resistance bacteria (ARBs) with cognate antibiotic resistance genes (ARGs) with clear implications for human health. In this context, MPs may be envisaged as hotspots and reservoirs of ARGs as selective enrichment on MPs of ARBs and ARGs has been reported; from an ecological point of view; horizontal transfer and spread of ARGs between bacteria may be facilitated by Class 1 integrons. Wang et al., 2020a, Wang et al., 2020b found an enrichment of ARGs and class 1 integron integrase gene (*intI1*) on MPs suggesting that *intI1* might facilitate the transmission of several ARGs through horizontal gene transfer between bacteria; pointing out to the role of MPs as mediators of microbial antibiotic resistance in the environment. In addition, if ingested, MPs might transport ARBs and cognate ARGs to different organisms changing gut microbiota and resistome (Laganà et al., 2019; Liu et al., 2021;

Martínez-Campos et al., 2021; Wang et al., 2020b; Xiang et al., 2019; Yang et al., 2019).

As indicated above, the plastisphere of polar regions has not been fully explored yet and many interesting questions remain to be answered: (i) Does the polar plastisphere differ from the microbial communities in the surrounding environment? (ii) Does it differ from the plastisphere recorded in other latitudes? (iii) How complex is the polar plastisphere? (iv) May MPs in polar regions be reservoirs of ARGs?

In an effort to answer those questions, in this work, we have characterized, for the first time, the polar plastisphere (bacteria, eukaryotes and fungi) on three types of MPs: poly-3-hydroxybutyrate (PHB), a biodegradable plastic, and two non-biodegradable plastic, low-density polyethylene (LDPE) and high-density polyethylene (HDPE). MPs were deployed as previously reported (Martínez-Campos et al., 2021) during 11 days into a shallow freshwater lake in the High Arctic in the surroundings of Ny-Ålesund (Svalbard, 78°N; 11°E), a coastal and summer ice-free area at Kongsfjorden (Svalbard Archipelago) where a previous study on the occurrence of MPs was done (González-Pleiter et al., 2020b). We hypothesized that the plastic material might select the associated plastisphere microbiome so that the associated microbiome might be different from that of microorganisms in the surrounding water and rock microbial mats (hereinafter MicMat). We also checked the presence of viable microorganisms within the characterized plastisphere. Finally, we hypothesized that MPs-colonizing bacteria might act as vectors of ARGs in polar environments by checking the relative abundance of *sulI* and *ermB* genes in bacteria attached to MPs as compared to those in the surrounding water and MicMat.

2. Materials and methods

2.1. Study area

The study area is an ephemeral shallow freshwater lake located near the international Arctic research base, Ny-Ålesund (Spitsbergen, Svalbard Archipelago; 78.94765° N, 11.81299° E, Fig. S1A). This lake with ca. ~0.75 m of maximum depth is fed by meltwater from glaciers and snowdrift and is surrounded by a variety of animal and plant species typical of the High Arctic ecosystems of Svalbard (Jiang et al., 2011; Kern et al., 2019; Fig. S1A). The benthic zone consists of hand-size rocks and pebbles (~10 × 10× 5 cm) covered by cohesive sediments.

2.2. Plastic polymers used for microbial colonization, ATR–FTIR spectral analysis and characterization of their surface properties

Three types of MPs were considered: poly-3-hydroxybutyrate (PHB), a biodegradable plastic (cylinders, 3–5 mm), and two non-biodegradable plastics: low-density polyethylene (LDPE) and high-

density polyethylene (HDPE), both spheres with 5 mm diameter. PHB was chosen because it is a biodegradable biopolymer that is considered one of the best candidates to replace current fossil-derived plastics. In the case of PE, both types are largely used in industry and have been found in several Arctic environments such as sediments (Bergmann et al., 2019), sub-surface water (La Daana et al., 2018), seawater (Lusher et al., 2015), sea ice (Obbard et al., 2014), benthic organisms (Fang et al., 2018) and seabirds (Amélineau et al., 2016). All MPs were obtained from Goodfellow Cambridge Ltd. (Huntingdon, England) and were additive-free.

To investigate potential weathering of MPs during the incubation time, the chemical composition of both, virgin (non-incubated) as well as the eleven-day incubated MPs, was analyzed by Attenuated Total Reflectance Fourier Transform Infrared (ATR-FTIR) spectral analysis. ATR-FTIR spectra were obtained in a Thermo-Scientific Nicolet iS10 apparatus with a Smart iTR-Diamond ATR module. Spectra were recorded using the following parameters: 20 scans, spectral range 500–4000 cm^{-1} and resolution of 4 cm^{-1}. For each MPs, five random spots were analyzed. Between samples, the ATR-crystal was cleaned with isopropanol and background signal updated. The spectra were analyzed with OMNIC version 9.1.26 (ThermoFisher Scientific Inc., Massachusetts, USA).

The determination of surface properties and microtexture of these MPs was done as previously reported by Martínez-Campos et al. (2021); briefly, the surface properties of the MPs were studied by contact angle measurements. Contact angles were determined with an optical contact angle meter (Krüss DSA25Drop Shape Analysis System) at room temperature using the sessile drop technique. Contact angles were measured using drops of MilliQ water, glycerol and diiodomethane delivered by the built-in syringe. Contact angle measurements were taken at least at three different positions for each solvent and material and analyzed using the software Drop Shape Analysis (DSA4) release 2.1. Surface tension was calculated using the procedure by Van Oss (2007). The procedure allowed obtaining the free energy of interaction between two identical surfaces immersed in a liquid, ΔG_{SWS}, which is a measure of the hydrophobicity or hydrophilicity of the surface. If $\Delta G_{SWS} > 0$, the surface is hydrophilic, whereas if $\Delta G_{SWS} < 0$, it is hydrophobic.

The microtexture of MPs was evaluated using a high-resolution 3D microscope with interferometry and profilometry model Leica DCM 8 with the analysis mode in confocal mode (green LED). The software used to process the result was Leica Scan version 6.5. The areas considered were 649 μm × 488 μm using three measurements per particle and three different particles. The measured parameters were the developed interfacial area ratio (Sdr) and kurtosis value (Sku). The Sdr parameter is expressed as the percentage of additional surface area contributed by the texture as compared to the planar definition area, the Sdr of a completely level surface is 0, but when a surface has any slope, its Sdr value becomes larger. The Sku value is a parameter of the sharpness of the surface height. Height normal distribution has a value of 3; a value of Sku less than 3 indicates that height distribution is skewed above the mean plane; on the contrary, Sku values higher than 3 indicates that its height distribution is spiked (high Sku values indicated a spiky surface, low Sku values indicates a bumpy surface) (Blunt and Jiang, 2003).

The Gibbs free energy of interaction, ΔG_{SWS}, and microtexture values are shown in Table S3. There were important differences in the surface properties of the three MPs. According to ΔG_{SWS}, hydrophobicity in increasing order was: PHB < LDPE < HDPE. Regarding microtexture, LDPE displayed the highest roughness (expressed as Sdr) mostly with ridge-and-valley appearance, PHB displayed intermediate roughness and uneven surfaces and HDPE had the flattest surface roughness. PHB and LDPE with kurtosis values (Sku > 3) showed spiked surfaces, while HDPE was softer.

2.3. Experimental design of MPs microbial colonization

The colonization experiment essentially followed the protocol developed by Martínez-Campos et al. (2021): The substrates were sterilized according to their properties: PHB was sterilized by autoclave (120 °C, 20 min); HDPE and LDPE with lower melting temperatures were sterilized using 10% hydrochloric acid 1 min and cleaning with sterilized Milli-Q water. Approximately, 8 g of each polymer type pellet were introduced into sterilized metallic cages with 1 mm holes by triplicate.

Metallic cages with MPs inside were deployed for eleven days (25/07/2017–4/08/2017) at a depth of 20 cm into the lake (Fig. S1B). After the incubation period -eleven days- (Fig. S1C), MPs were carefully extracted from the metallic cages to avoid the destruction of the biofilm and the residual water of the sample dried with sterilized filter; the high water surface tension and hydrophobicity of the substrates precluded the removal of the attached biofilm (Epstein et al., 2011; Pompilio et al., 2008). Dried MPs were placed into sterile tubes and stored at -20 °C until DNA extraction.

In addition, 1170 mL of water (three replicates) were filtered by 0.22 μm membrane Millipore filter and also stored at -20 °C until DNA extraction in order to obtain a representative sample of the microbial community in the surrounding water. Three representative rocks (~10 × 10 × 5 cm) were collected from the bottom of the lake and wrapped with aluminum foil previously heated to 200 °C for 2 h; rocks were stored at -20 °C until DNA extraction in order to obtain a representative sample of the microbial community thriving in the sediment.

As procedural control, a metallic cage with each type of MPs was exposed to the same experimental conditions (sterilized, transported, dried with sterilized filter paper, placed into sterile tubes and stored at -20 °C) except for the incubation. This was done both at time 0 and after the eleven-day incubation period. Thus, these MPs (hereinafter referred to as control) were also extracted from their metallic cages on 4/08/2017, dried with sterilized filter paper, placed into sterile tubes, and stored at -20 °C until DNA extraction.

2.4. Scanning electron microscope (SEM) imaging of microbial colonizers

The morphological characterization of microbial colonizers attached to MPs was performed by SEM using a Zeiss DSM 950 equipped with Quartz PCI software for analysis and image capture. For SEM examination, six MP particles of each MP type were thawed, dried for 12 h under sterile conditions, and metalized with a gold layer of 3 nm using a metallizer Polaron model SC7640. In addition, two MP particles of each type from the procedural controls were also examined and no microbial colonizers were found (data not shown).

2.5. Viability analysis of MPs microbial colonizers

The viability of the microorganisms attached to MPs was studied using the cell-permeable 5-Cyano-2,3-Ditolyl Tetrazolium Chloride (CTC) redox dye. This dye is reduced from the soluble colorless form into its corresponding fluorescent insoluble formazan visualized as intracellular opaque dark-red deposits under transmitted illumination, or as red fluorescent spots (excitation and emission maxima at 488 and 630 nm, respectively). SYBR Green (Molecular Probes; excitation and emission maxima at 488 and 510 nm, respectively) was used for specific staining of nucleic acids. Red fluorescence autofluorescence associated with chlorophyll fluorescence (excitation and emission maxima at 488 and 680 nm, respectively) was to visualize microalgae. Epifluorescence images were taken using a Zeiss AxioImager M2 microscope (Carl Zeiss, Germany). Details on staining procedures can be found elsewhere (Tashyreva et al., 2013).

Fluorescence microscopy allowed cell counting to estimate the total and viable microbial colonizers on each of the MP substrates. Means and standard deviation values were calculated for each MP from six MP particles of each type. Furthermore, three MP particles of each type from the procedural controls were studied and no microbial colonizers were found on them (data not shown).

2.6. Microbial diversity analysis

2.6.1. DNA extraction

DNA was extracted with the phenol-chloroform method from all frozen samples (MPs, water filters, and microbial mats from rocks) in triplicate. The procedure was essentially as described by Martínez-Campos et al.

(2021). Pellets of each plastic substrate were distributed in three 2 mL Eppendorf tubes. Water filters were cut into small fragments with sterilized scissors and distributed in three 1.5 mL Eppendorf tubes. Rocks were scraped using a sterilized scalpel, separating the biofilm from the substrate, which was transferred to 2 mL Eppendorf tubes. The procedure started with the addition of Tris-HCL 10 mM, EDTA 0.1 mM pH 7.5, 0.05% SDS (W/V) and 0.01% of silica pellets (W/V) to the samples. After that, 0.5 volumes of hot phenol ultrapure pH 7.9 (65 °C) was added, and the samples were vortexed and warmed to 65 °C for 1 min three times to fully release the DNA from the samples. Subsequently, 0.5 volume of chloroform was added, samples were vortexed and frozen again six times. Finally, samples were centrifuged at 13000 rpm at 4 °C for 20 min. 1 volume of hot phenol pH 7.9 (65 °C) was added to the supernatant (which was transferred to a new Eppendorf tube) which was subsequently centrifuged at 13000 rpm at 4 °C for 20 min. This was repeated twice. Finally, all supernatants that belonged to the same sample were pooled and 2 volumes of absolute ethanol were added, samples were mixed and frozen at -20 °C overnight to precipitate the DNA. Samples were centrifuged at 13000 rpm at 4 °C for 20 min. The supernatant was discarded, and the pellet was washed with 1 volume of 70% ethanol to remove the salts. Samples were further centrifuged at 13000 rpm at 4 °C for 2 min. Finally, samples were dried, and the DNA was resuspended in 40 μL of Milli-Q water. All samples were stored at -20 °C.

2.6.2. DNA sequencing

PCR amplifications of the 16S rRNA, 18S rRNA, and ITS regions of each sample (MPs, water filters, and microbial mats from rocks) (Table S1) were carried out by the Genomics Service of Parque Científico de Madrid (Madrid, Spain). The specific primers used are also shown in Table S1. DNA libraries and amplicon sequencing were performed essentially as previously described (Martínez-Campos et al., 2021; Martinez-Campos et al., 2018); briefly, PCR products were purified and Miseq (Illumina) libraries were prepared according to manufacturer's instructions. DNA libraries were checked for size, concentration and integrity using a Bioanalyzer (Agilent). Amplicon sequencing was performed using an Illumina Miseq sequencer. Paired - end reads (2 × 300) were generated according to manufacturer's instructions obtaining at least 100,000 reads per replicate. The Knudsenheia lake water samples were sequenced on a separate run.

2.6.3. Data analysis

Reads were processed using the DADA2 pipeline v.1.14.1 (Callahan et al., 2016). Primers (Table S1) were trimmed, as proposed by the authors, using the trimLeft option. Runs were quality filtered separately per primer set, allowing for a run-specific error correction. Parameter maxee was adjusted per run and per amplicon set to obtain a comparable number of

reads between runs, and was set as a default at c(2,2) for the forward and reverse reads for the incubated and sediment samples (all primer sets), and at c(4,5) for 18S rRNA and at c(5,6) for both 16S rRNA and ITS of the Knudsenheia lake water samples. Both runs were then processed further together using the default pipeline, including chimera removal using the removeBimeraDenovo command with the consensus method. ASV reads were then classified using the rdp classifier (Wang et al., 2007) implemented in Mothur v.1.42.1 (Schloss et al., 2009), using databases PR^2 v.4.12 (Guillou et al., 2012) for 18S rRNA, Greengenes v.13.8 (DeSantis et al., 2006) for 16S rRNA and UNITE v. 04.02.2020 (Nilsson et al., 2019) for ITS.

Downstream analyses were performed in R v.3.6.2 (R Core Team, 2019). Some taxa were removed a priori. These were Embryophyceae and Metazoa in the 18S rRNA dataset, mitochondria, chloroplasts and Archaea in the 16S rRNA dataset, and all non-Fungi in the ITS dataset. Strict singletons, i.e. occurring with only 1 read in the entire dataset, were removed as well.

CAP analysis (canonical analysis of principal coordinates) was performed on Hellinger transformed data with the CAPdiscrim function from package Biodiversity R v.2.12.3 (Kindt and Coe, 2005) using the Bray-Curtis dissimilarity and allowing a maximum of 10 PCoA axes to be considered for the best classification success. Indicator species analysis was performed with package Indic species v.1.7.9 (Cáceres and Legendre, 2009). Venn-diagrams were made with package Venn Diagram v1.6.20 (Chen, 2018) on non-subsampled samples grouped per substrate type, after which aggregated groups were subsampled to the lowest number of reads in any group. Lastly, PERMANOVA was performed using the Adonis function with default settings in vegan v.2.5.7 (Oksanen et al., 2013), while pairwise PERMANOVA was performed using package pairwise Adonis v.0.0.1 (Martinez, 2017) with Holm correction for multiple testing.

2.6.4. Accession numbers

Sequences used in this study were submitted to NCBI under the Bioproject number: PRJNA722376.

2.7. Relative abundance of ARGs

The relative abundance of two ARGs (*sulI* and *ermB*) in the microbial communities attached to MPs, MicMat and microorganisms in the surrounding water were evaluated by quantitative PCR. *sulI* confers resistance to sulfonamides and *ermB* confers resistance to macrolides. These ARGs have been previously detected in the same area (Tan et al., 2018) and in other Arctic regions (Hayward et al., 2018; McCann et al., 2019). Assays were carried out in a LightCycler® 480 (Roche; USA) system using LightCycler® 480SYBR Green I Master (Roche; USA). The primers used are shown in Table S2. Quantitative PCR conditions included a pre-

amplification step (8 cycles and 60 °C) using 1 ng of template DNA quantified by PicoGreen fluorescent stain and subsequently an initial denaturation step at 95 °C for 5 min, followed by 40 cycles: denaturation (95 °C) and annealing/elongation (60 °C). Three technical replicates were run for each gene and each sample obtaining in each one a detectable cycle threshold (Ct) value. Both positive and negative controls were included in every run. The $2^{-\Delta\Delta T}$ method was used to normalize values relative to the 16S gene of the same sample (Livak and Schmittgen, 2001).

3. Results

3.1. Visualization of microbial colonizers attached to MPs

SEM images revealed the presence of whole microbial cells on all MPs incubations after eleven days (Fig. 1 and Fig. S2). These cells were observed both inside cavities (Fig. 1A and B; Fig. S2A, C, D, E and F) and attached to the surface of MPs (Fig. 1C and D; Fig. S2B, G, H, I, J). In general, a large diversity of microorganisms and shapes were visible on the MPs including typical morphotypes of algae (Fig. 1A), filamentous cyanobacterial-like cells (Fig. 1B), both spherical and filamentous bacteria (Fig. 1C) and a wide variety of diatoms (Fig. 1D and Fig. S2). These morphological characteristics of the cells suggested the presence of both eukaryotic (Fig. 1A and D) as well as prokaryotic (Fig. 1B and C) organisms.
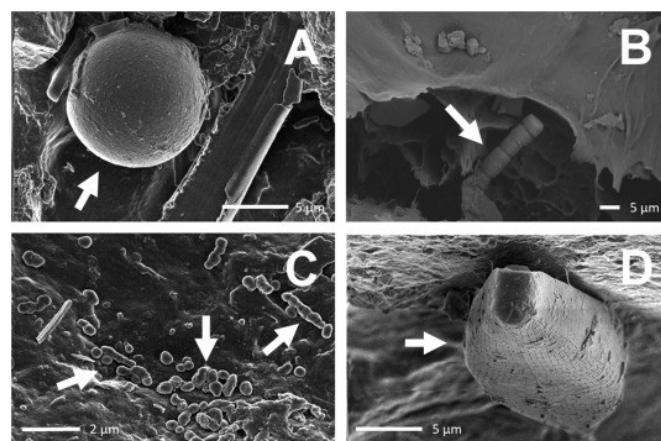
Figure 1: Scanning electron microscope (SEM) images of microbial colonizers on MPs incubated for eleven days in an Arctic freshwater lake: Arrows indicate: A) putative alga B) putative filamentous cyanobacterium C) bacterial cells and D) diatom.

The eleven-day incubation period did not result in any appreciable weathering of MPs as evidenced by ATR–FTIR spectral analysis (Fig. S4). No differences were observed in the peaks of any of the three polymer types in virgin vs. incubated MPs. The spectra of LDPE and HDPE revealed the main features of polyethylene. The stretching vibrations of $-CH_2$ appeared at 2915 cm^{-1} and 2848 cm^{-1}, the bending of $-CH_2$ at 1465 cm^{-1}, and the
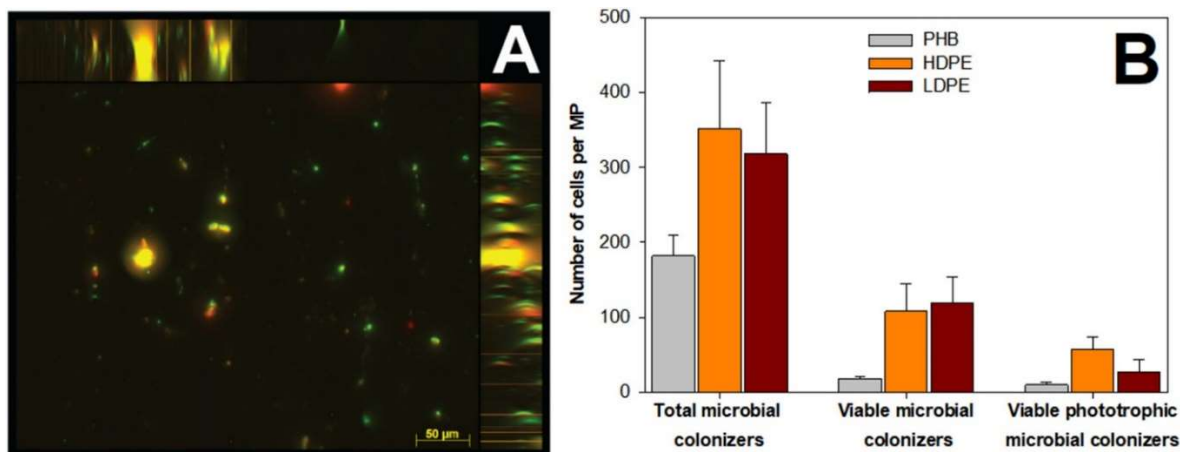
Figure 2: Viability of the microbial colonizers. (A) Representative fluorescence microscopy image of a MP incubated for eleven days in an Arctic freshwater lake. Green dots indicate the presence of DNA. Orange dots indicate active cells. Yellow dots indicate the presence of both DNA and active cells. Scale bar equal 50 μm. (B) Total and viable microbial colonizers found on MP surface, which were incubated for eleven days in the lake.

rocking vibration of -CH$_2$ at 719 cm^{-1}. The bending of -CH$_3$ terminal groups corresponding to the branching of LDPE appeared at 1365 cm^{-1} in LDPE (not in HDPE due to the absence of branching). The spectra of PHB showed the vibrations of carbonyl groups in the backbone at 1719 cm^{-1}, the C-O stretching bands at 1277 and 1044 cm^{-1}, the C-H bending vibrations at 1455 and 1377 cm^{-1}, and the CH stretching bands at 2867 and 2934 cm^{-1}.

3.2. Viability of MPs microbial colonizers

The viability of microbial colonizers was analyzed using two fluorochromes SYBR-Green and CTC, which allowed simultaneous assessment of cell numbers on each MP as well as their metabolic activity. Those cells displayed with green fluorescence (SYBR-Green +) were defined as microbial colonizers attached to MPs, while those simultaneously presenting bright orange/yellow CTF fluorescence (SYBR-Green+/CTC+) were metabolically active (Fig. 2A). Cells associated with red autofluorescence (chlorophyll +) were defined as phototrophic microbial colonizers (i.e. unicellular algae and cyanobacteria). Thus, fluorescence microscopy images show viable microbial colonizers attached to the different MPs assayed. Cell counts revealed that each MP contained between 351 ± 91 and 182 ± 28 microbial colonizers depending on the type of plastic (Fig. 2B). The counts also showed that all MPs exhibited viable microbial colonizers ranging from 120 ± 33 to 18 ± 3 (Fig. 2B). Also, viable phototrophs were also found attached to all MPs (Fig. 2B). About a third of the microbial colonizers found in each MP was metabolically active (37.7 ± 10.5% on LDPE, 30.5 ± 10.7% on HDPE and 9.9 ± 5.5% on PHB).

3.3. Sequence yield and quality

About 3,766,153 reads were obtained using Illumina sequencing from which 1,219,758 reads corresponded to 16S rRNA gene, 1,284,113 reads to 18S rRNA gene and 1,262,282 reads to the ITS region. After quality filtration and chimera removal 1,168,661 reads of 16S rRNA gene, 1,127,928 reads of 18S rRNA gene and 572,974 reads of ITS remained for downstream analyses. The rarefaction curves for all samples (Fig. S3) approached the saturation plateau, pointing out that the libraries were adequately sampled. Samples were subsampled to the lowest number of reads in a sample for each dataset as follows: 18789 reads for 16S rRNA dataset, 9202 reads for 18S rRNA dataset, and 2375 reads for ITS region dataset. Based on 97% sequence similarity, these sequences could be clustered into 6682 ASVs for prokaryotes (16S rRNA), 1571 ASVs for eukaryotes (18S rRNA) and 251 ASVs for fungi (ITS).

3.4. α-Diversity analysis

Microbial α-diversity was estimated using the Shannon Index (Fig. 3). Regarding prokaryotes (Fig. 3A), MicMat presented significantly (Tukey's HSD test; p-value < 0.05) higher Shannon Index values (6.32 ± 0.21) than MPs. MPs had a significant (Tukey's HSD test; p-value < 0.05) higher value of Shannon index (4.96 ± 0.28) than that of the surrounding water (2.37 ± 0.25; Fig. 3). No significant (Tukey's HSD test; p-value > 0.05) differences were found between non-biodegradable MPs (5.05 ± 0.23) and biodegradable MPs (4.77 ± 0.10).

In the case of eukaryotes (Fig. 3B), MPs had a significantly higher Shannon Index value (3.20 ± 0.73; Tukey's HSD test; p-value < 0.05) than that of the surrounding water (1.57 ± 0.07). No significant (Tukey's HSD test; p-value > 0.05) differences were found between MPs and MicMat (4.27 ± 0.45) or between non-biodegradable MPs (3.04 ± 0.84) and biodegradable MPs (3.52 ± 0.33). For fungi (Fig. 3C), the diversity for targeting ITS region revealed that MPs showed significantly (Tukey's HSD test; p-value <0.05) higher Shannon Index value (2.82 ± 0.45) than that of the surrounding water (1.61 ± 0.49) and MicMat (1.78 ± 0.58).
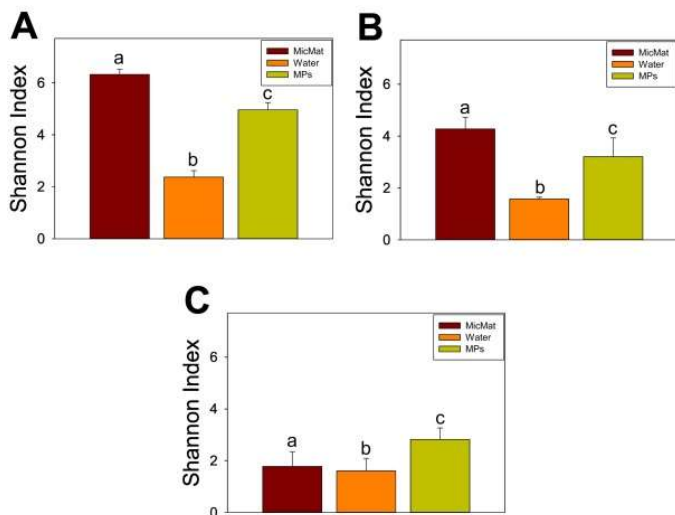
Figure 3: α-diversity values using the Shannon-Wienner index of prokaryotes (A), eukaryotes (B) and fungi (C) in all the substrates assayed: MPs, surrounding water and MicMat of Knudsenheia pond (Ny-Ålesund, Svalbard). Lowercase letters indicated significant differences between substrates in the Tukey's HSD test to prokaryotes (16S rRNA), eukaryotes (18S rRNA) and fungi (ITS). Statistical significance was a p-value <0.05.

There were differences in microbial community changes according to substrates but also microorganisms; in the case of bacteria, MicMat showed the highest diversity followed by MPs and surrounding water, which revealed a less diverse bacterial community. Regarding eukaryotes, MicMat showed a slightly, although non-significant, higher diversity than MPs and water also showed the least diversity in the eukaryotic community. However, for fungi, MPs showed the highest diversity of the tested substrates. It is also remarkable that no significant differences were observed in community diversity in biodegradable (PHB) versus non-biodegradable MPs (HDPE and LDPE).

3.5. β-Diversity

The CAP analyses based on ASVs revealed a pattern of clustering structure for prokaryotes (Fig. S5) and eukaryotes (Fig. S6) according to each type of substrates (MicMat, surrounding water and MPs) finding a very clear differentiation in the distance on the Y axis between MPs and surrounding water. It should be noted that MPs were also clearly separated from MicMat according to the X and Y axis. In the case of fungi (Fig. S7), a clear differentiation in the distance on the X axis were observed between MPs and surrounding water and MicMat.

The differences among the MPs, surrounding water and MicMat were essentially confirmed by pairwise PERMANOVA tests (Table S4). In this regard, the differences in prokaryotic composition were significant between MPs and MicMat (pairwise PERMANOVA, p-value < 0.05) and MPs and surrounding water (pairwise PERMANOVA, p-value < 0.05). Pairwise

PERMANOVA analyses revealed significant differences (p-value < 0.05) between biodegradable (PHB) and non-biodegradable MPs, between biodegradable and natural environment (surrounding water plus MicMat) and between non-biodegradable and natural environment, too. However, no statistically significant differences were found in the pairwise PERMANOVA comparisons of polymer types or between individual polymer types and surrounding water or MicMat (Table S4).

Similarly, the eukaryotic community displayed significant differences between MPs and MicMat (pairwise PERMANOVA, p-value < 0.05) and the MPs compared to the surrounding water per taxa abundances (pairwise PERMANOVA, p-value < 0.05). Statistically significant differences were found in the pairwise PERMANOVA comparisons, in terms of surface description, between biodegradable and natural environment (surrounding water plus MicMat) and between non-biodegradable and natural environment; however, no significant differences were found between polymer types or between individual polymer types and surrounding water or MicMat (Table S4).

Regarding fungi, when the ITS region assemblages were compared regarding the different substrates, only MPs and MicMat displayed significant differences (pairwise PERMANOVA; p-value < 0.05). No statistically significant differences were found in the pairwise PERMANOVA comparisons in terms of surface description: between biodegradable (PHB) and non-biodegradable MPs, between biodegradable and natural environment (surrounding water plus MicMat) and between non-biodegradable and natural environment, or between polymer types or between individual polymer types and surrounding water or MicMat (Table S4).

Altogether, the data point to clear differences in community composition between MPs and surrounding water and between MicMat and MPs particularly in terms of prokaryotic and eukaryotic assemblages (pairwise PERMANOVA; p-value < 0.05).

Venn diagrams were generated to help visualize dissimilarity among microbial communities from tested substrates (Fig. 4). It shows the number of unique as well as overlapping OTUs significantly differentiated across substrates. Unique ASVs were found in all substrates. For prokaryotes and eukaryotes, the highest number of unique ASVs was associated with MicMat (prokaryotic: 1979 ASVs; eukaryotic: 345 ASVs) followed by LDPE (prokaryotic: 769 ASVs; eukaryotic: 413 ASVs), HDPE (prokaryotic: 623 ASVs; eukaryotic: 206 ASVs) and PHB (prokaryotic: 606 ASVs; eukaryotic: 205 ASVs). The lowest number of unique ASVs was associated with surrounding water (prokaryotic: 33 ASVs; eukaryotic: 148 ASVs).
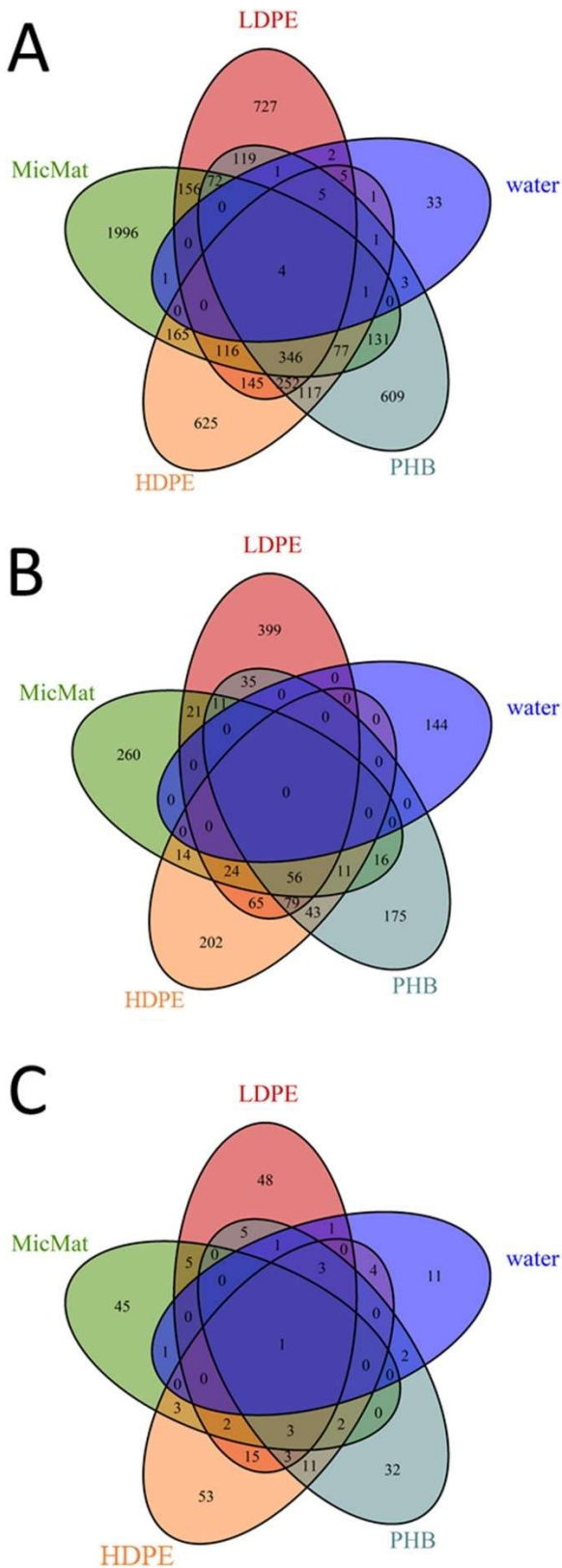
Figure 4: Venn diagrams showing the unique and shared fraction of prokaryotes (A), eukaryotes (B) and fungi (C) ASVs on MP substrates (LDPE, HDPE and PHB), ASVs in the surrounding water (water) and ASVs in the microbial mats in rocks (MicMat).

In the case of fungi, the highest number of unique ASVS was associated with both PEs (53 ASVs HDPE; 47 ASVs LDPE) followed by MicMat (44 ASVs) andPHB (32 ASVs). The lowest number of unique ASVs was associated with surrounding water too (11

ASVs). Thus, the highest number of unique ASVs was associated with MicMat except for fungi, which seems logical since the rock microbial mat is probably the most stable community core. Nevertheless, the lowest number of unique ASVs was associated with surrounding water in all cases.

MPs, MiCMat and surrounding water had 4 ASVs in common (3 prokaryotic ASVs; and 1 fungal ASV). Regarding MPs and their surrounding environment (MicMat and water), 9 ASVs (6 prokaryotic ASVs and 3 fungal ASVs) were shared between MPs and surrounding water while 437 ASVs (376 prokaryotic ASVs; 58 eukaryotic ASVs and 3 fungal ASVs) were shared between MPs and MicMat. In this regard, 183 ASVs (164 prokaryotic ASVs; 16 eukaryotic ASVs and 3 fungal ASVs) were shared by HDPE and MicMat whereas 169 ASVs (140 prokaryotic ASVs; 24 eukaryotic: ASVs and 5 fungal ASVs) were shared by LDPE and MicMat but only 149 ASVs (127 prokaryotic ASVs and 22 eukaryotic ASVs) were shared by PHB and MicMat. The high number of overlaps between MPs and MicMat might indicate that MicMat, rather than the surrounding water, could be considered as the main source of microorganisms that colonized MPs.

When considering only polymer type, 306 ASVs were shared between the three MPs (223 prokaryotic ASVs; 80 eukaryotic ASVs and 3 fungal ASVs) with a high number of ASVs shared by both PEs, HDPE and LDPE, which amounted to 234 ASVs (153 prokaryotic ASVs; 66 eukaryotic ASVs and 15 fungal ASVs).

3.6. Microbial community composition

The bar charts represented in Fig. 5 shows the prokaryotic (A), eukaryotic (B) and fungal (C) distribution at the phylum level associated to the different tested substrates: MPs (PHB, HDPE and LDPE), surrounding water and MicMat.

Regarding bacteria, taxonomic analysis of 16S rRNA genes showed that the majority of the reads in the sample set were associated with the phyla Proteobacteria with 64.8% relative abundance followed by Bacteroides (15.7%) and Cyanobacteria (8.4%) (Fig. 5A). In terms of relative abundances and predominant phyla, the bacterial community composition was very similar between MPs and MicMat: Proteobacteria (76.1%), Cyanobacteria (7.9%), Bacteroidetes (6.3%), Actinobacteria (3.1%) and Verrucomicrobia (2.3%) were the most abundant phyla in MPs; similarly, Proteobacteria (41.9%), Cyanobacteria (18.9%), Bacteroidetes (16.9%), Planctomycetes (5.7%) and Verrucomicrobia (4.3%) predominated in MicMat. Proteobacteria (53.5%), Bacteroidetes (42.6%) and Actinobacteria (2.8%) were the most abundant in surrounding water.

Table S5 shows the specific core microbial assemblages on the tested substrates at a genus-level resolution

8
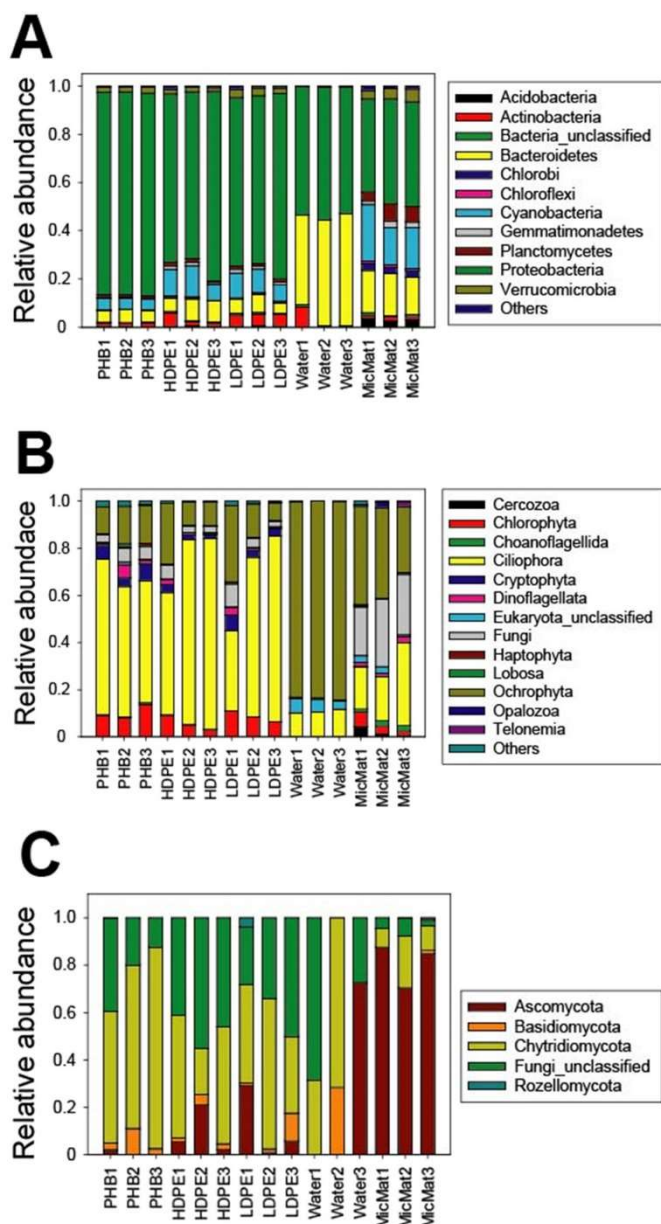
Figure 5: Relative abundance of prokaryotes (A), eukaryotes (B) and fungi (C) at the phylum level associated to the different substrates: MPs (PHB, HDPE and LDPE), surrounding water (water) and MicMat (the three replicates of each substrate are included). Others are phyla whose representation is less than 1%.

based on relative taxa abundance ≥1%. Bacterial community composition at this level was clearly different between the tested substrates. In general, MPs were characterized by a high abundance of *Mycoplana* (24.8%), followed by *Erythromicrobium* (6.3%), Comamonadaceae_unclassified (4.6%), *Rhodobacter* (4.1%), *Rhodoferax* (2.9%), Moraxellaceae_unclassified (2.7%), Sphingomonadaceae_unclassified (2.6%) and *Zymomonas* (2.5%). It is noteworthy that there were differences in the relative abundance of some genera between biodegradable (PHB) and non-biodegradable (HDPE and LDPE) MPs (Table S5). In both, non-biodegradable and biodegradable MPs, genus *Mycoplana* clearly predominated (25% and 24.4%, respectively). Regarding other genera, non-

biodegradable MPs were characterized by, in order of decreasing abundance, *Erythromicrobium* (7.6%), *Rhodobacter* (4.5%), Comamonadaceae_unclassified (4.0%), Sphingomonadaceae_unclassified (2.7%), *Zymomonas* (2.5%), *Pseudanabaena* (2.2%) and *Sphingomonas* (2.1%) whereas biodegradable MPs were characterized by, in order of decreasing abundance, Moraxellaceae_unclassified (8.1%), *Rhodoferax* (6.0%), Comamonadaceae_unclassified (5.8%), *Polaromonas* (4.0%), *Erythromicrobium* (3.7%), *Rhodobacter* (3.2%) and *Zymomonas* (2.5%). Regarding MicMat, a different set of genera composed by *Rhodobacter* (6.9%), *Gloeobacter* (6.4%), Acetobacteraceae_unclassified (3.8%), Chitinophagaceae_unclassified (3.6%), *Leptolyngbya* (3.4%), Saprospiraceae_unclassified (3.2%), Bacteroidetes_unclassified (3.1%), Alphaproteobacteria_unclassified (2.6%), *Pseudanabaena* (2.4%), Comamonadaceae_unclassified (2.3%) predominated. Surrounding water was characterized by a high abundance of *Polynucleobacter* (28.4%) and *Flavobacterium* (26.2%), followed by *Limnohabitans* (14.2%) Cytophagaceae_unclassified (12.9%), Sphingomonadaceae_unclassified (9.4%), ACK-M1_unclassified (2.8%), *Fluviicola* (1.6%) and *Sediminibacterium* (1.5%). It is relevant that there were significant (PERMANOVA; *p*-value < 0.05) differences in the relative abundance of some of the above described genera between MPs, surrounding water and MicMat. In this sense, the relative abundance of *Mycoplana*, *Erythromicrobium*, *Rhodoferax*, *Zymomonas*, *Polaromonas*, *Novosphingobium*, *Leptothrix* and *Hydrogenophaga* was significantly (PERMANOVA; *p*-value < 0.05) higher in MPs than in surrounding water and MicMat. Regarding prokaryotic primary producers (Cyanobacteria), the relative abundance of *Synechococcus*, *Limnococcus*, *Nodosilinea* and *Snowella* was significantly (PERMANOVA; *p*-value < 0.05) higher in MPs than in surrounding water and MicMat.

Taxonomic analysis of 18S rRNA genes (Fig. 5B) revealed that the majority of the reads in the sample set were associated with the phyla Ciliophora (44.6%), Ochrophyta (33.4%), Fungi (7.9%), Chlorophyta (5.7%) and Cryptophyta (2.5%). The most abundant phyla in MPs were Ciliophora (62.8%), Ochrophyta (15.9%), Chlorophyta (8.2%), Fungi (4.7%), Cryptophyta (4.1%) and Dinoflagellata (1.7%). The most abundant phyla in MicMat were Ochrophyta (36.0%), Fungi (25.1%), Ciliophora (23.8%), Chlorophyta (3.9%), Cercozoa (2.1%), Dinoflagellata (1.9%) and Choanoflagellida (1.9%). The most abundant phyla in surrounding water were Ochrophyta (83.5%), Ciliophora (10.8%) and Eukaryota_unclassified (4.9%) (Fig. 5B).

At genus-level resolution (Table S5), eukaryotic community composition was clearly different between the tested substrates, MPs were characterized by a high

abundance of *Stentor* (45.9%), followed by *Vorticella* (7.5%), Chrysophyceae_Clade-C_unclassified (3.9%), *Cryptomonas* (3.8%), *Uroleptus* (3.5%), *Tetraselmis* (2.9%), *Epipyxis* (2.7%), Sessilida_unclassified (2.6%), Chrysophyceae_X_unclassified (1.9%), Chytridiomycetes_unclassified (1.5%), Chilodonellidae_unclassified (1.5%), *Chrysophyceae_Clade-D* (1.5%) and *Chlamydomonas* (1.4%). Genus *Stentor* was clearly dominant in both non-biodegradable (53.8%) as well as biodegradable MPs (30.2%); however, regarding other genera, some slight differences in relative abundances were found between non-biodegradable and biodegradable MPs: *Epipyxis* (4.0%), *Vorticella* (3.9%), Chrysophyceae_Clade-C_unclassified (3.5%), *Uroleptus* (3.4%), *Cryptomonas* (3.0%) and Chrysophyceae_X_unclassified (2.2%) predominated in non-biodegradable MPs whereas *Vorticella* (14.6%), *Cryptomonas* (5.5%), *Tetraselmis* (5.0%), Chrysophyceae_Clade-C_unclassified (4.8%), Sessilida_unclassified (4.0%), *Uroleptus* (3.7%) and Chilodonellidae_unclassified (2.9%) dominated in biodegradable MPs. The genera that predominated in MicMat were Pezizomycotina_unclassified (12.3%), *Navicula* (9.9%), *Stentor* (5.9%), *Phaeoplaca* (5.4%), Chytridiomycetes_unclassified (3.9%), *Staurosira* (3.8%), Ophryoglenida_unclassified (3.1%), Sessilida_unclassified (3.0%), *Rhizophydium* (2.7%) and Chrysophyceae_X_unclassified (2.3%). Surrounding water was mainly dominated by *Chrysophyceae_Clade-C_unclassified* (82.1%), followed by *Strombidiida_A_XX* (7.8%), and Hypotrichia_unclassified (1.8%). It is relevant that there were significant (PERMANOVA; *p*-value < 0.05) differences in the relative abundance of some of the above described genera between MPs, surrounding water and MicMat. In this context, the relative abundance of *Stentor*, *Vorticella*, *Cryptomonas*, *Uroleptus*, *Tetraselmis*, *Epipyxis*, *Chrysophyceae_Clade-D*, *Chlamydomonas*, *Monoraphidium*, *Diatoma*, *Cosmarium*, *Chrysophyceae_Clade-B2*, *Oocystis* and *Fragilaria* was significantly (PERMANOVA; *p*-value < 0.05) higher in MPs than in surrounding water and MicMat.

In the case of fungi (ITS) (Fig. 5C), 28.9% of ASVs could not be identified (35.9% on MPs, 4.8% in MicMat and 32% in surrounding water). The majority of the reads in the sample set were associated with Chytridiomycota (40.7%), Ascomycota (25.4%) and Basidiomycota (4.6%). The most relevant differences at the phyla level were between MPs and MicMat as MPs were characterized by a high abundance of the phyla Chytridiomycota (52.0%), followed by Ascomycota (7.3%), Basidiomycota (4.3%) while the most abundant phyla in MicMat were Ascomycota (81%) and Chytridiomycota (13.3%). The relative abundances in surrounding water were: Chytridiomycota (34.4%), Ascomycota (24.2%) and Basidiomycota (9.5%).

At genus-level resolution (Table S5), MPs showed a higher abundance of *Betamyces* (22.2%), Chytridiomycota_unclassified (19.9%), Chytridiomycota_ unclassified (7.2%), Didymellaceae_unclassified (2.4%), *Cryptococcus* (1.4%), *Arrhenia* (1.2%), *Paranamyces* (1.0%) and Polychytriales_unclassified (1.0%). The predominant genus in both non-biodegradable and biodegradable MPs was *Betamyces* (17.6% and 31.4%, respectively). Nevertheless, there were some interesting differences in the relative abundance of some other genera such as *Cryptococcus* (1.7%), *Paranamyces* (1.5%) and *Xylodon* (1.0%) which were present on non-biodegradable MPs but absent in biodegradable MPs whereas *Arrhenia* (3.6%) and *Malassezia* (1%) were present in biodegradable but absent in non-biodegradable MPs. Regarding MicMat, Ascomycota_unclassified (49.2%), Helotiales_unclassified (31.1%), Chytridiomycota_unclassified (8.7%) and *Betamyces* (3.6%) were the most abundant genera. Surrounding water was characterized by the high abundance of *Betamyces* (23.5%), followed by *Cladosporium* (20.2%), *Xylodon* (7.1%), Chytridiomycota_ unclassified (6.2%), Saccharomycetales_unclassified (3.7%), Chytridiomycota_unclassified (3.3%) and *Cortinarius* (2,4%). For fungi, no significant differences (PERMANOVA; *p*-value < 0.05) in the relative abundance at genus-level resolution were found between MPs, surrounding water and MicMat, probably, due to the limitations in fungal ASVs identification.

3.7. Relative abundance of ARGs *ermB* and *sulI*

Fig. 6 shows the relative abundance of *ermB* and *sulI* ARGs on the tested plastic substrates, surrounding water and MicMat. *ermB* was not detected in the MicMat; the *ermB* gene (Fig. 6A) was detected on biofilms attached to all three plastic substrates with higher abundance in HDPE, followed by PHB and almost undetectable in LDPE; however, this ARG was far more abundant in surrounding water than in the MP substrates. Regarding the *sulI* gene (Fig. 6B), it was also detected in higher relative abundance in HDPE, followed by PHB and LDPE as compared to surrounding water and MicMat where it was barely detectable. Results indicated that bacteria attached to plastics harbored both ARGs and that those attached to HDPE showed the highest abundance of both ARGs. It also should be noticed that in the case of the *sulI* gene, it concentrated mostly on bacteria attached to MPs when compared to bacteria in surrounding water or those attached to the MicMat.

4. Discussion

In the present study and to our knowledge, this is the first study of microbial assemblages (plastisphere) of MPs, biodegradable (PHB) and non-biodegradable (HDPE and LDPE), in Arctic freshwaters. There have
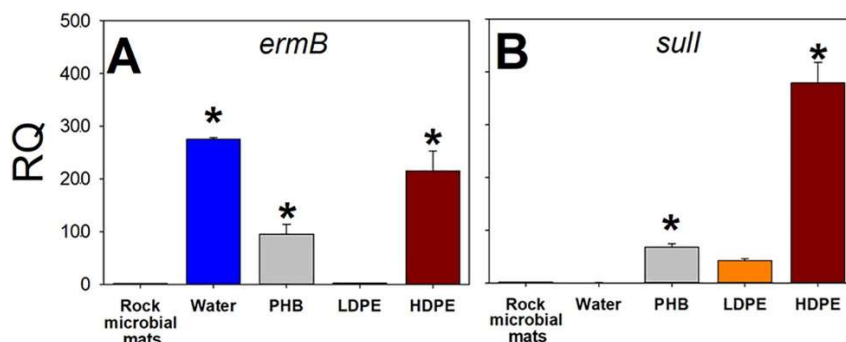
Figure 7: Relative abundance of *ermB* (A) and *sulI* (B) genes in bacteria measured in the surrounding water (water), MicMat, and MPs. Error bars indicate standard deviations of triplicates. Asterisk (*) denotes a statistically significant difference between the relative abundance of *ermB* and *sulI* genes in the MicMat and surrounding water and MPs (KruskalWallis test; p-value <0.05).

been few previous studies of microbial assemblages on MPs in polar regions, mostly marine environments (Amaral-Zettler et al., 2020; Caruso, 2020). Regarding the Arctic, there is one study on microbial colonization

not on MPs but on stainless steel surfaces which was related to biocorrosion of this specific material in natural seawater, also tested in Ny-Ålesund (Amaral-Zettler et al., 2020; Caruso, 2020; Scotto et al., 1986) and there is one report on the plastisphere microbiome of Arctic soils (Rüthi et al., 2020).

Nowadays, plastics and MPs in particular are widely recognized as a new niche for a plethora of microorganisms (Amaral-Zettler et al., 2020; Rogers et al., 2020; Wright et al., 2021) including bacteria, archaea, eukaryotes such as fungi, protists and small animals like bryozoans. All these organisms form a unique and diverse community, which shows different types of nutrition and complex trophic relationships between them: Autotrophy, heterotrophy, symbiosis, predation, parasitism and pathogenesis. MPs may concentrate nutrients that favor microbial metabolism and may enhance viability of bacteria in oligotrophic environments (Webb et al., 2008); our study confirmed that about a third of microbial colonizers were viable. Most studies indicate that plastisphere differs from the microbial communities of surrounding water, soil, sewage/sediment, as well as those of other substrates like wood or glass and usually show a higher alpha diversity (Martínez-Campos et al., 2021; Wright et al., 2021; Yi et al., 2021; Zhang et al., 2019; Zhao et al., 2021). Core microbiomes on specific plastic substrates could be defined (De Tender et al., 2017; Ogonowski et al., 2018; Webb et al., 2008). Differences between substrates might be stronger during early stages of biofilm formation (Oberbeckmann et al., 2016); in this context, Martínez-Campos et al. (2021) identified early-colonization core microbiomes on seven different types of MPs (including biodegradable as well as non-biodegradable ones) suggesting that each polymer type might select early attachment of distinctive bacteria. Buoyancy of plastics may behave as rafts in transporting and spreading plastics along aquatic ecosystems (Amaral-Zettler et al., 2020; Mincer et al., 2016; Wright et al., 2021); however, not all plastics are

buoyant, some sink or remain neutrally buoyant, being density the driver of buoyancy (Reisser et al., 2014). Turbulence is a main factor, at least in the ocean, that can vertically mix buoyant plastics and vertical mixing may affect their numbers, mass and size distribution (Reisser et al., 2014). Plastisphere may also have a key role in plastics buoyancy and vertical distribution in the water column; as calculated by Morét-Ferguson et al. (2010), the microbial biomass attached to marine plastic debris may be above 6% of the total mass of a piece of MP. The plastisphere may increase density of plastics and MPs and contribute to their sinking at the bottom of the ocean (Mincer et al., 2016).

Our results indicate that complex microbial assemblages are formed on the MPs, which are different from those in the surrounding water, and those in the microbial mats of rocks sampled at the bottom of the Arctic shallow freshwater lake. In general, we found a slightly higher richness in the microbial mats of the rocks in the sediment as compared to the ASV richness in biofilms of MPs; nevertheless, higher richness was found on MPs as compared to that of the surrounding lake water. Previous studies in freshwater and marine aquatic environments have also found differences, particularly, in bacterial species richness since eukaryotes have been seldom included in the studies, between MPs and surrounding water, finding in general lower richness on plastics with respect to the water (Amaral-Zettler et al., 2015; Ogonowski et al., 2018; Zettler et al., 2013); however, there are a few studies which have found just the opposite with higher bacterial species richness in MPs as compared to the surrounding water (Frère et al., 2018; McCormick et al., 2014; Peng et al., 2018). Recently, Martínez-Campos et al. (2021) also found that MPs had higher bacterial diversity than WWTP effluent water free-living bacteria; the authors studied the early colonization phase (48 h) and suggested that this could be explained by the active adhesion of first bacterial colonizers, facilitating the adhesion of new species from the water column in the first hours of biofilm formation. In this context, our results are even more relevant as they include microbial mats on sediment rocks as well as surrounding water for comparison indicating that species richness is

significantly higher in biofilms, either on MPs or sediment rocks, as compared to the surrounding water. In addition, our study has included not only bacterial communities but also eukaryotes and fungi confirming that the plastisphere may be a complex ecosystem of bacteria, protists, fungi and small animals like bryozoans which interact in a variety of ways and are glued together within a matrix composed of extracellular polymeric substances (EPS; Amaral-Zettler et al., 2020).

An interesting question is whether the composition of the complex plastisphere found on MPs is essentially different to that of microbial communities of other substrates (sediment rocks) or the surrounding water and whether specific assemblages are formed between particular members of bacteria with co-associated eukaryotes and fungi. For example, diatoms which are recognized among first colonizers in marine biofilm formation and may be envisaged as pioneer species that may facilitate subsequent heterotrophic microbial colonization; Amin et al. (2012) reported that diatoms can form specific assemblages with co-associated bacterial epibionts including *Alteromonas, Pseudoalteromonas, Roseobacter* and the Flavobacteriaceae *Tenacibacumum* and *Polaribacter* (Abell and Bowman, 2005).

β- Diversity analysis indicated remarkable differences in the community composition, particularly regarding bacteria and eukaryotes, between the three substrates: MPs, MicMat and surrounding water. Based on relative abundances, core microbiomes (bacteria, eukaryotes and fungi) could be assigned to each tested substrate (Table S5). The differences in the relative abundance of some genera between biodegradable (PHB) and non-biodegradable (HDPE and LDPE) MPs could probably be due to the different surface properties of the polymers (Table S3). The results of this study could be very useful to identify specific assemblages of co-existing taxa of different biological organization and a frame to study the potentially complex interaction between them, i.e. symbiosis or predation. MPs-core microbiomes have been identified before both in freshwater and marine environments but solely concerning prokaryotes (De Tender et al., 2017; Martínez-Campos et al., 2021; McCormick et al., 2014; McCormick et al., 2016; Oberbeckmann et al., 2018; Ogonowski et al., 2018; Peng et al., 2018).

Phyla Proteobacteria, Cyanobacteria, Bacteroidetes, Actinobacteria and Verrucomicrobia dominated MPs biofilms. Alpha and gammaproteobacteria as well as Bacteroidetes are early colonizers and are known to produce the EPS (Dang and Lovell, 2000). Actinobacteria as well as Bacteroidetes may have a role in organic matter processing which helps in biofilm conditioning that facilitates the attachment of other organisms (Kirchman, 2002). Same phyla were also highly abundant in MicMat on sediment rocks as the

process of biofilm formation may be quite similar to that on MPs.

It is noteworthy that the bacterial communities of the MPs were characterized by a high relative abundance of the genera *Mycoplana*, *Erythromicrobium* and *Rhodoferax*, whereas these showed low abundance in water and MicMat. It is relevant that these genera have species with the capacity to metabolize recalcitrant substances and their presence has been reported in polar regions as well as in freshwaters (Baker et al., 2017; Brinda Lakshmi et al., 2012; Maltman and Yurkov, 2018; Niederberger et al., 2015; Tahon and Willems, 2017; Velan et al., 2012). Other bacterial genera that appeared in MPs and have been identified in polar regions are *Rhodobacter* (Crisafi et al., 2016)*, Polaromonas* (Gawor et al., 2016), *Zymomonas* (Wang et al., 2020b), *Flavobacterium* (Chaudhary et al., 2020), *Sphingomonas* (Jang and Lee, 2016) and *Pseudanabaena* (Khan et al., 2019). Bacteria present in these cryoenvironments could have biotechnological potential (i.e. polymer and other recalcitrant molecules bioremediation) as they may possess special adaptations and particular sets of genes as already pointed out by Rüthi et al. (2020).

Cyanobacteria are relevant photosynthetic representatives that together with diatoms and other algae (see below) contribute to net primary production on any biofilm. Filamentous genera, including *Phormidium*, *Rivularia* and *Leptolyngbya*, have been reported in marine environments on MPs (Amaral-Zettler et al., 2020; Bryant et al., 2016). In our colonization experiment, some cyanobacterial genera *Synechococcus*, *Limnococcus*, *Nodosilinea* and *Snowella*, were significantly more abundant in MPs. It is noteworthy that other cyanobacterial genera were also present at relatively higher abundance in MicMat [*Gloeobacter*, *Leptolyngbya* and *Pseudanabaena* the latter also present at the same relative abundance in MPs, Table S5], as the colonization experiment took place in a shallow lake.

The eukaryotic communities of the MPs were characterized by a significant high relative abundance of some of the genera of the ciliates such as *Stentor*, *Vorticella* and *Uroleptus*, and the algae *Cryptomonas*, *Chlamydomonas*, *Tetraselmis* and *Epipyxis*, whereas these genera showed low abundance in surrounding water and MicMat. In the case of *Stentor* its relative abundance was eight-fold higher in MPs than MicMat, which could be related to the significant high relative abundance of some genera of algae; *Cryptomonas*, *Tetraselmis*, *Epipyxis, Chlamydomonas Monoraphidium, Diatoma, Cosmarium, Chrysophyceae_Clade-B2_X, Oocystis and Fragilaria*), on MPs as compared to their relative abundance in the surrounding water and MicMat. As these are filter feeders that normally display selective feeding behaviors on algae (Kim et al., 2007), a predator-prey relationship may be relevant between the ciliates and

12

the algae living together on the microbial assemblages on MPs (Table S5).

Diatoms (phylum Ochrophyta) were clearly seen in the SEM images of colonized MPs. Most studies have reported diatoms as early and even dominant colonizers on MPs (Amaral-Zettler et al., 2020; Eich et al., 2015; Kettner et al., 2019). Although microscopic studies, as observed in our study, have indicated that diatoms are common members of the plastisphere, metagenomic studies have reported that diatom taxa have a low relative abundance in the eukaryotic community, which suggests that they may be replaced over time as biofilm matures (Amaral-Zettler et al., 2020; Kettner et al., 2019).

Regarding fungal communities, it is noteworthy that Arctic-colonized MPs were characterized by a high abundance of the phyla Chytridiomycota that has been found to dominate fungal assemblages on polyethylene and polystyrene substrates in brackish and freshwaters (Kettner et al., 2019). In this study, fungal reads contributed up to 4% of the total eukaryotic reads; in our study and according to 18S rRNA reads, fungi represented up to 7.9%; nevertheless, it should be noticed that fungal diversity in the plastisphere remains poorly known (Amaral-Zettler et al., 2020). In our study, the most abundant genera were Betamyces, *Cryptococcus*, *Arrhenia* and *Paranamyces* whereas these genera showed low abundance in surrounding water and MicMat (Table S5). The genus *Paranayces* and *Betamyces*, two species of *Arrhenia* (*A. auriscalpium* and *A. lobata*, which is an obligate parasite of wet mosses) and several species of *Cryptococcus* have been previously described in polar regions (Butinar et al., 2007; Cripps et al., 2006; da Silva et al., 2021; Singh and Singh, 2012; Zhang et al., 2016). It should be noted that some species (*C. neoformans* and *C. gatti)* of the Cryptococcus are invasive fungi that cause cryptococcosis even in northern regions such as Vancouver Island, Canada. (Kidd et al., 2004). The role of saprotrophs such as fungi on MPs microbial assemblages may include decomposition, parasitism, predation, symbiosis and pathogenesis. In addition, it is noteworthy that many fungi can degrade complex carbon polymers such as lignin by using enzymes such as oxidases, laccases and peroxidases, which have also been reported as responsible for the degradation of plastic polymers by fungi (Shah et al., 2007).

There is growing evidence that MPs might be reservoirs and hot spots of ARGs (for a recent review, see (Liu et al., 2021). Our study showed that the *ermB* ARG was detected on biofilms attached to all three MPs with higher relative abundance in HFPE and PHB; this gene was below the detection limit in MicMat but was much more abundant in surrounding water than in any of the plastic substrates. The *sulI* ARG was mostly found in MPs, also in higher abundance in HDPE followed by PHB. Therefore, both ARGs were detected in MPs and

mainly concentrated in HDPE. Other authors have already found that different types of MPs concentrate a number of ARGs (Martínez-Campos et al., 2021; Wang et al., 2020b; Yang et al., 2019); as MPs are transported even long distances through different environmental compartments (Koelmans et al., 2016; Schwarz et al., 2019), they help to disseminate ARGs globally, even to remote polar regions as found in this study, with the subsequent effect in the long-term for human health. ARGs may be transferred from one bacterium to another by horizontal gene transfer and Class I integrons may have a crucial role in that transfer; *SulI* genes are part of the 3′ conserved segments of Class 1 integrons (Carattoli, 2001; Lucey et al., 2000; Zhao et al., 2001). Regarding MPs, Wang et al., (2020) found a significant correlation between ARGs and class 1 integron integrase gene (*intI1*) and suggested that *intI1* could make easier the transmission of several ARGs such as *sulI*, *tetX*, *ermE* and *ermF* between water and MPs through horizontal gene transfer indicating a role of MPs in the spreading of antibiotic resistance in the environment. Finally and regarding antibiotic resistance dissemination in Polar Regions, some of the bacterial genera identified in this study as abundant members of microbial assemblages on MPs such as *Erythromicrobium* have been found to be resistant to several antibiotics including penicillin, tetracycline, streptomycin, polymyxin B, bacitracin and kanamycin. Furthermore, *Mycoplana* appears to be a potential microorganism able to degrade ampicillin (Wang et al., 2017). In the case of *Rhodoferax*, some of the species of this genus have RND and ABC efflux systems, which play a prominent role in acquired antibiotic resistance and the species (Jin et al., 2020) *Rhodoferax antarcticus*, which was isolated from a microbial mat in an Antarctic pond, has genes for resistance to beta-lactam antibiotic (Baker et al., 2017).

5. Conclusions

Plastisphere was compared with microbial communities of surrounding water and microbial mats (MicMat) on sediment rocks in a shallow Arctic lake. Diversity was higher in MicMat and MPs than in the surrounding water.

Significant differences were found in the community composition of bacteria and eukaryotes in the three substrates: MPs, MicMat and surrounding water. Specific microbiomes were assigned to each of the three substrates suggesting complex relationships between co-existing taxa (i.e. predator-prey) that are worthy of further investigation.

Some of the bacterial genera found on MPs were clearly characteristic of polar regions and genera such as *Mycoplana*, *Erythromicrobium* and *Rhodoferax* have species able to metabolize recalcitrant substances. These cryophilic bacteria might have biotechnological interest due to their special adaptations to polar environments.

ermB and *sulI* ARGs were enriched on MPs, particularly on HDPE; this may be a concern regarding human health since ARGs may be transferred between bacteria by horizontal gene transfer with subsequent dissemination of ARGs due to transport of MPs between different environmental compartments.

The fact that ARGs have been found on MPs even in a pristine remote freshwater lake in the Arctic raises awareness about the importance of correct waste management and clean-up protocols to protect polar regions which are threatened by the global dissemination of MPs.

Acknowledgements

References

Abell, G., Bowman, J.P., 2005. Colonization and community dynamics of class Flavobacteria on diatom detritus in experimental mesocosms based on Southern Ocean seawater. FEMS Microbiol. Ecol. 53, 379–391.

Agathokleous, E., Iavicoli, I., Barceló, D., Calabrese, E.J., 2021. Ecological risks in a 'plastic'world: a threat to biological diversity? J. Hazard. Mater. 417, 126035.

Amaral-Zettler, L.A., Zettler, E.R., Slikas, B., Boyd, G.D., Melvin, D.W., Morrall, C.E., et al., 2015. The biogeography of the Plastisphere: implications for policy. Front. Ecol. Environ. 13, 541–546.

Amaral-Zettler, L.A., Zettler, E.R., Mincer, T.J., 2020. Ecology of the plastisphere. Nat. Rev. Microbiol. 18, 139–151.

Amélineau, F., Bonnet, D., Heitz, O., Mortreux, V., Harding, A.M., Karnovsky, N., et al., 2016. Microplastic pollution in the Greenland Sea: background levels and selective contamination of planktivorous diving seabirds. Environ. Pollut. 219, 1131–1139.

Amin, S.A., Parker, M.S., Armbrust, E.V., 2012. Interactions between diatoms and bacteria. Microbiol. Mol. Biol. Rev. 76, 667–684.

Baker, J.M., Riester, C.J., Skinner, B.M., Newell, A.W., Swingley, W.D., Madigan, M.T., et al., 2017. Genome sequence of *Rhodoferax antarcticus* ANT. BRT; a psychrophilic purple nonsulfur bacterium from an Antarctic microbial mat. Microorganisms 5, 8.

Barrows, A., Cathey, S.E., Petersen, C.W., 2018. Marine environment microfiber contamination: global patterns and the diversity of microparticle origins. Environ. Pollut. 237, 275–284.

Bergmann, M., Wirzberger, V., Krumpen, T., Lorenz, C., Primpke, S., Tekman, M.B., et al., 2017. High quantities of microplastic in Arctic deep-sea sediments from the HAUSGARTEN observatory. Environ. Sci. Technol. 51, 11000–11010.

Bergmann, M., Mützel, S., Primpke, S., Tekman, M.B., Trachsel, J., Gerdts, G., 2019. White and wonderful? Microplastics prevail in snow from the Alps to the Arctic. Sci. Adv. 5, eaax1157.

Blunt, L., Jiang, X., 2003. Advanced Techniques for Assessment Surface Topography: Development of a Basis for 3D Surface Texture Standards" Surfstand": Elsevier.

Bourdages, M.P., Provencher, J.F., Baak, J.E., Mallory, M.L., Vermaire, J.C., 2021. Breeding seabirds as vectors of microplastics from sea to land: evidence from colonies in Arctic Canada. Sci. Total Environ. 764, 142808.

Brinda Lakshmi, M., Muthukumar, K., Velan, M., 2012. Immobilization of mycoplana sp. mvmb2 isolated from petroleum contaminated soil onto papaya stem (*Carica papaya L.*) and its application on degradation of phenanthrene. CLEAN–Soil, Air, Water 40, 870–877.

Bryant, J.A., Clemente, T.M., Viviani, D.A., Fong, A.A., Thomas, K.A., Kemp, P., et al., 2016. Diversity and activity of communities inhabiting plastic debris in the North Pacific Gyre. MSystems 1.

Butinar, L., Spencer-Martins, I., Gunde-Cimerman, N., 2007. Yeasts in high Arctic glaciers: the discovery of a new habitat for eukaryotic microorganisms. Antonie Van Leeuwenhoek 91, 277–289.

Cáceres, M.D., Legendre, P., 2009. Associations between species and groups of sites: indices and statistical inference. Ecology 90, 3566–3574.

Callahan, B.J., McMurdie, P.J., Rosen, M.J., Han, A.W., Johnson, A.J.A., Holmes, S.P., 2016. DADA2: high-resolution sample inference from Illumina amplicon data. Nat. Methods 13, 581–583.

Carattoli, A., 2001. Importance of integrons in the diffusion of resistance. Vet. Res. 32, 243–259.

Caruso, G., 2020. Microbial colonization in marine environments: overview of current knowledge and emerging research topics. J. Mar. Sci. Eng. 8, 78.

Chaudhary, D.K., Dahal, R.H., Kim, D.-U., Kim, J., 2020. *Flavobacterium sandaracinum* sp. nov., *Flavobacterium caseinilyticum* sp. nov., and *Flavobacterium hiemivividum* sp. nov., novel psychrophilic bacteria isolated from Arctic soil. Int. J. Syst. Evol. Microbiol. 70, 2269–2280.

Chen, H., 2018. VennDiagram: generate high-resolution Venn and Euler plots. R package version 1.6. 20. https://CRAN.R-project.org/package=VennDiagram.

Cincinelli, A., Scopetani, C., Chelazzi, D., Lombardini, E., Martellini, T., Katsoyiannis, A., et al., 2017. Microplastic in the surface waters of the Ross Sea (Antarctica): occurrence, distribution and characterization by FTIR. Chemosphere 175, 391–400.

Cózar, A., Martí, E., Duarte, C.M., García-de-Lomas, J., Van Sebille, E., Ballatore, T.J., et al., 2017. The Arctic Ocean as a dead end for floating plastics in the North Atlantic branch of the Thermohaline Circulation. Sci. Adv. 3, e1600582.

Cripps, C.L., Horak, E., Boertmann, D., Knudsen, H., 2006. *Arrhenia auriscalpium* in arcticalpine habitats: world distribution, ecology, new reports from the southern Rocky Mountains, USA. Arctic Alpine Micol. 6, 17–24.

Crisafi, F., Giuliano, L., Yakimov, M.M., Azzaro, M., Denaro, R., 2016. Isolation and degradation potential of a cold-adapted oil/PAH-degrading marine bacterial consortium from Kongsfjorden (Arctic region). Rendiconti Lincei 27, 261–270.

Dang, H., Lovell, C.R., 2000. Bacterial primary colonization and early succession on surfaces in marine waters as determined by amplified rRNA gene restriction analysis and sequence analysis of 16S rRNA genes. Appl. Environ. Microbiol. 66, 467–475.

De Tender, C., Devriese, L.I., Haegeman, A., Maes, S., Jr, Vangeyte, Cattrijsse, A., et al., 2017. Temporal dynamics of bacterial and fungal colonization on plastic debris in the North Sea. Environ. Sci. Technol. 51, 7350–7360.

DeSantis, T.Z., Hugenholtz, P., Larsen, N., Rojas, M., Brodie, E.L., Keller, K., et al., 2006. Greengenes, a chimera-checked 16S rRNA gene database and workbench compatible with ARB. Appl. Environ. Microbiol. 72, 5069–5072.

Ding, Y., Zou, X., Wang, C., Feng, Z., Wang, Y., Fan, Q., et al., 2021. The abundance and characteristics of atmospheric microplastic deposition in the northwestern South China Sea in the fall. Atmos. Environ. 253, 118389.

Eich, A., Mildenberger, T., Laforsch, C., Weber, M., 2015. Biofilm and diatom succession on polyethylene (PE) and biodegradable plastic bags in two marine habitats: early signs of degradation in the pelagic and benthic zone? PLoS One 10, e0137201.

Epstein, A.K., Pokroy, B., Seminara, A., Aizenberg, J., 2011. Bacterial biofilm shows persistent resistance to liquid wetting and gas penetration. Proc. Natl. Acad. Sci. 108, 995–1000.

Fang, C., Zheng, R., Zhang, Y., Hong, F., Mu, J., Chen, M., et al., 2018. Microplastic contamination in benthic organisms from the Arctic and sub-Arctic regions. Chemosphere 209, 298–306.

Fang, C., Zheng, R., Hong, F., Jiang, Y., Chen, J., Lin, H., et al., 2021. Microplastics in three typical benthic species from the Arctic: occurrence, characteristics, sources, and environmental implications. Environ. Res. 192, 110326.

Fei, Y., Huang, S., Zhang, H., Tong, Y., Wen, D., Xia, X., et al., 2020. Response of soil enzyme activities and bacterial communities to the accumulation of microplastics in an acid cropped soil. Sci. Total Environ. 707, 135634.

Frère, L., Maignien, L., Chalopin, M., Huvet, A., Rinnert, E., Morrison, H., et al., 2018. Microplastic bacterial communities in the Bay of Brest: influence of polymer type and size. Environ. Pollut. 242, 614–625.

García-López, E., Rodríguez-Lorente, I., Alcázar, P., Cid, C., 2019. Microbial communities in coastal glaciers and tidewater tongues of Svalbard Archipelago, Norway. Front. Mar. Sci. 5, 512.

Gawor, J., Grzesiak, J., Sasin-Kurowska, J., Borsuk, P., Gromadka, R., Górniak, D., et al., 2016. Evidence of adaptation, niche separation and microevolution within the genus Polaromonas on Arctic and Antarctic glacial surfaces. Extremophiles 20, 403–413.

González-Pleiter, M., Edo, C., Velázquez, D., Casero-Chamorro, M.C., Leganés, F., Quesada, A., Fernández-Piñas, F, Rosal, R., 2020a. First detection of microplastics in the freshwater of an Antarctic Specially Protected Area. Mar. Pollut. Bull. 161, 111811.

González-Pleiter, M., Velázquez, D., Edo, C., Carretero, O., Gago, J., Barón-Sola, Á., Hernández, L.E., Yousef, I., Quesada, A., Leganés, F., Rosal, R., Fernández-Piñas, F., 2020b. Fibers spreading worldwide: microplastics and other anthropogenic litter in an Arctic freshwater lake. Sci. Total Environ. 722, 137904.

González-Pleiter, M., Edo, C., Aguilera, Á., Viúdez-Moreiras, D., Pulido-Reyes, G., GonzálezToril, E., Osuna, S., de Diego-Castilla, G., Leganés, F., Fernández-Piñas, F., Rosal, R., 2021. Occurrence and transport of microplastics sampled within and above the planetary boundary layer. Sci. Total Environ. 761, 143213.

Granberg, M., von Friesen, L.W., Bach, L., Collard, F., Gabrielsen, G.W., Strand, J., 2019. Anthropogenic Microlitter in Wastewater and Marine Samples From Ny-Ålesund. Barentsburg and Signehamna, Svalbard.

Guillou, L., Bachar, D., Audic, S., Bass, D., Berney, C., Bittner, L., et al., 2012. The Protist Ribosomal Reference database (PR2): a catalog of unicellular eukaryote small sub-unit rRNA sequences with curated taxonomy. Nucleic Acids Res. 41, D597–D604.

Hayward, J.L., Jackson, A.J., Yost, C.K., Hansen, L.T., Jamieson, R.C., 2018. Fate of antibiotic resistance genes in two Arctic tundra wetlands impacted by municipal wastewater. Sci. Total Environ. 642, 1415–1428.

Hoellein, T., Rojas, M., Pink, A., Gasior, J., Kelly, J., 2014. Anthropogenic litter in urban freshwater ecosystems: distribution and microbial interactions. PLoS One 9, e98485.

Huntington, A., Corcoran, P.L., Jantunen, L., Thaysen, C., Bernstein, S., Stern, G.A., et al., 2020. A first assessment of microplastics and other anthropogenic particles in Hudson Bay and the surrounding eastern Canadian Arctic waters of Nunavut. Facets 5, 432–454.

Imran, M., Das, K.R., Naik, M.M., 2019. Co-selection of multi-antibiotic resistance in bacterial pathogens in metal and microplastic contaminated environments: an emerging health threat. Chemosphere 215, 846–857.

Jang, S.-H., Lee, C., 2016. Gene cloning and characterization of a psychrophilic phthalate esterase with organic solvent tolerance from an Arctic bacterium *Sphingomonas glacialis* PAMC 26605. J. Mol. Catal. B Enzym. 133, S337–S345.

Jiang, S., Liu, X., Sun, J., Yuan, L., Sun, L., Wang, Y., 2011. A multi-proxy sediment record of late Holocene and recent climate change from a lake near Ny-Ålesund, Svalbard. Boreas 40, 468–480.

Jin, C.-Z., Zhuo, Y., Wu, X., Ko, S.-R., Li, T., Jin, F.-J., et al., 2020. Genomic and Metabolic Insights into Denitrification, Sulfur Oxidation, and Multidrug Efflux Pump Mechanisms in the Bacterium *Rhodoferax sediminis* sp. nov. Microorganisms 8, 262.

Kern, R., Hotter, V., Frossard, A., Albrecht, M., Baum, C., Tytgat, B., et al., 2019. Comparative vegetation survey with focus on cryptogamic covers in the high Arctic along two differing catenas. Polar Biol. 42, 2131–2145.

Kettner, M.T., Oberbeckmann, S., Labrenz, M., Grossart, H.-P., 2019. The eukaryotic life on microplastics in brackish ecosystems. Front. Microbiol. 10, 538.

Khan, Z., Maznah, W.W., Merican, M.F., Convey, P., Najimudin, N., Alias, S.A., 2019. A comparative study of phycobilliprotein production in two strains of Pseudanabaena isolated from Arctic and tropical regions in relation to different light wavelengths and photoperiods. Polar Sci. 20, 3–8.

Kidd, S.E., Hagen, F., Tscharke, R., Huynh, M., Bartlett, K.H., Fyfe, M., et al., 2004. A rare genotype of Cryptococcus gattii caused the cryptococcosis outbreak on Vancouver Island (British Columbia, Canada). Proc. Natl. Acad. Sci. 101, 17258–17263.

Kim, Y.-O., Chang, M., Ka, S.-K., Han, M.-S., 2007. Grazing on Algae and Growth of the Freshwater Heterotrich Ciliate *Stentor Roeselii*. J. Freshwater Ecol. 22, 2, 2007.

Kindt, R., Coe, R., 2005. Tree Diversity Analysis: A Manual and Software for Common Statistical Methods for Ecological and Biodiversity Studies: World Agroforestry Centre.

Kirchman, D.L., 2002. The ecology of Cytophaga–Flavobacteria in aquatic environments. FEMS Microbiol. Ecol. 39, 91–100.

Kirstein, I.V., Kirmizi, S., Wichels, A., Garin-Fernandez, A., Erler, R., Löder, M., et al., 2016. Dangerous hitchhikers? Evidence for potentially pathogenic Vibrio spp. on microplastic particles. Mar. Environ. Res. 120, 1–8.

Koelmans, A.A., Bakir, A., Burton, G.A., Janssen, C.R., 2016. Microplastic as a vector for chemicals in the aquatic environment: critical review and model-supported reinterpretation of empirical studies. Environ. Sci. Technol. 50, 3315–3326.

Kühn, S., Schaafsma, F.L., van Werven, B., Flores, H., Bergmann, M., Egelkraut-Holtus, M., et al., 2018. Plastic ingestion by juvenile polar cod (*Boreogadus saida*) in the Arctic Ocean. Polar Biol. 41, 1269–1278.

La Daana, K.K., Gårdfeldt, K., Lyashevska, O., Hassellöv, M., Thompson, R.C., O'Connor, I., 2018. Microplastics in sub-surface waters of the Arctic Central Basin. Mar. Pollut. Bull. 130, 8–18.

La Daana, K.K., Gardfeldt, K., Krumpen, T., Thompson, R.C., O'Connor, I., 2020. Microplastics in sea ice and seawater beneath ice floes from the Arctic Ocean. Sci. Rep. 10, 1–11.

Laganà, P., Caruso, G., Corsi, I., Bergami, E., Venuti, V., Majolino, D., et al., 2019. Do plastics serve as a possible vector for the spread of antibiotic resistance? First insights from bacteria associated to a polystyrene piece from King George Island (Antarctica). Int. J. Hyg. Environ. Health 222, 89–100.

Lamb, J.B., Willis, B.L., Fiorenza, E.A., Couch, C.S., Howard, R., Rader, D.N., et al., 2018. Plastic waste associated with disease on coral reefs. Science 359, 460–462.

Liu, Y., Liu, W., Yang, X., Wang, J., Lin, H., Yuyi, Y., 2021. Microplastics are a hotspot for antibiotic resistance genes: progress and perspective. Sci. Total Environ. 145643.

Livak, K.J., Schmittgen, T.D., 2001. Analysis of relative gene expression data using realtime quantitative PCR and the 2- $\Delta\Delta$CT method. Methods 25, 402–408.

Lucey, B., Crowley, D., Moloney, P., Cryan, B., Daly, M., O'Halloran, F., et al., 2000. Integronlike structures in Campylobacter spp. of human and animal origin. Emerg. Infect. Dis. 6, 50.

Lusher, A.L., Tirelli, V., O'Connor, I., Officer, R., 2015. Microplastics in Arctic polar waters: the first reported values of particles in surface and sub-surface samples. Sci. Rep. 5, 1–9.

Ma, H., Pu, S., Liu, S., Bai, Y., Mandal, S., Xing, B., 2020. Microplastics in aquatic environments: toxicity to trigger ecological consequences. Environ. Pollut. 261, 114089.

Maltman, C., Yurkov, V., 2018. Bioremediation potential of bacteria able to reduce high levels of selenium and tellurium oxyanions. Arch. Microbiol. 200, 1411–1417.

Martínez, Arbizu P., 2017. pairwiseAdonis: Pairwise Multilevel Comparison Using Adonis. R Package Version 0.0. 1.

Martínez-Campos, S., Redondo-Nieto, M., Shang, J., Peña, N., Leganés, F., Rosal, R., Fernández-Piñas, F., 2018. Characterization of microbial colonization and diversity in reverse osmosis membrane autopsy. Desalin. Water Treat. 131, 9–29.

Martínez-Campos, S., González-Pleiter, M., Fernández-Piñas, F., Rosal, R., Leganés, F., 2021. Early and differential bacterial colonization on microplastics deployed into the effluents of wastewater treatment plants. Sci. Total Environ. 757, 143832.

McCann, C.M., Christgen, B., Roberts, J.A., Su, J.-Q., Arnold, K.E., Gray, N.D., et al., 2019. Understanding drivers of antibiotic resistance genes in High Arctic soil ecosystems. Environ. Int. 125, 497–504.

McCormick, A., Hoellein, T.J., Mason, S.A., Schluep, J., Kelly, J.J., 2014. Microplastic is an abundant and distinct microbial habitat in an urban river. Environ. Sci. Technol. 48, 11863–11871.

McCormick, A.R., Hoellein, T.J., London, M.G., Hittie, J., Scott, J.W., Kelly, J.J., 2016. Microplastic in surface waters of urban rivers: concentration, sources, and associated bacterial assemblages. Ecosphere 7, e01556.

Mincer, T.J., Zettler, E.R., Amaral-Zettler, L.A., 2016. Biofilms on plastic debris and their influence on marine nutrient cycling, productivity, and hazardous chemical mobility. Hazardous Chemicals Associated With Plastics in the Marine Environment. Springer, pp. 221–233.

Morét-Ferguson, S., Law, K.L., Proskurowski, G., Murphy, E.K., Peacock, E.E., Reddy, C.M., 2010. The size, mass, and composition of plastic debris in the western North Atlantic Ocean. Mar. Pollut. Bull. 60, 1873–1878.

Morgana, S., Ghigliotti, L., Estévez-Calvar, N., Stifanese, R., Wieckzorek, A., Doyle, T., et al., 2018. Microplastics in the Arctic: a case study with sub-surface water and fish samples off Northeast Greenland. Environ. Pollut. 242, 1078–1086.

Niederberger, T.D., Sohm, J.A., Gunderson, T.E., Parker, A.E., Tirindelli, J., Capone, D.G., et al., 2015. Microbial community composition of transiently wetted Antarctic Dry Valley soils. Front. Microbiol. 6, 9.

Nilsson, R.H., Larsson, K.-H., Taylor, A.F.S., Bengtsson-Palme, J., Jeppesen, T.S., Schigel, D., et al., 2019. The UNITE database for molecular identification of fungi: handling dark taxa and parallel taxonomic classifications. Nucleic Acids Res. 47, D259–D264.

Obbard, R.W., Sadri, S., Wong, Y.Q., Khitun, A.A., Baker, I., Thompson, R.C., 2014. Global warming releases microplastic legacy frozen in Arctic Sea ice. Earth's Future 2, 315–320.

Oberbeckmann, S., Osborn, A.M., Duhaime, M.B., 2016. Microbes on a bottle: substrate, season and geography influence community composition of microbes colonizing marine plastic debris. PLoS One 11, e0159289.

Oberbeckmann, S., Kreikemeyer, B., Labrenz, M., 2018. Environmental factors support the formation of specific bacterial assemblages on microplastics. Front. Microbiol. 8, 2709.

Ogonowski, M., Motiei, A., Ininbergs, K., Hell, E., Gerdes, Z., Udekwu, K.I., et al., 2018. Evidence for selective bacterial community structuring on microplastics. Environ. Microbiol. 20, 2796–2808.

Oksanen, J., Blanchet, F.G., Kindt, R., Legendre, P., Minchin, P.R., O'hara, R., et al., 2013. Package 'vegan'. Community Ecology Package, Version. 2 pp. 1–295.

van Oss, C.J., 2007. Development and applications of the interfacial tension between water and organic or biological surfaces. Colloids Surf. B: Biointerfaces 54, 2–9.

Peeken, I., Primpke, S., Beyer, B., Gütermann, J., Katlein, C., Krumpen, T., et al., 2018. Arctic sea ice is an important temporal sink and means of transport for microplastic. Nat. Commun. 9, 1–12.

Peng, Y., Li, J., Lu, J., Xiao, L., Yang, L., 2018. Characteristics of microbial community involved in early biofilms formation under the influence of wastewater treatment plant effluent. J. Environ. Sci. 66, 113–124.

Perini, L., Gostinčar, C., Gunde-Cimerman, N., 2019. Fungal and bacterial diversity of Svalbard subglacial ice. Sci. Rep. 9, 1–15.

Pompilio, A., Piccolomini, R., Picciani, C., D'Antonio, D., Savini, V., Di Bonaventura, G., 2008. Factors associated with adherence to and biofilm formation on polystyrene by *Stenotrophomonas maltophilia*: the role of cell surface hydrophobicity and motility. FEMS Microbiol. Lett. 287, 41–47.

Poon, F.E., Provencher, J.F., Mallory, M.L., Braune, B.M., Smith, P.A., 2017. Levels of ingested debris vary across species in Canadian Arctic seabirds. Mar. Pollut. Bull. 116, 517–520.

R Core Team, 2019. R: a language and environment for statistical computing. R Foundation for Statistical Computing. Austria, Vienna https://www.R-project.org/.

Redondo-Hasselerharm, P., Gort, G., Peeters, E., Koelmans, A., 2020. Nano-and microplastics affect the composition of freshwater benthic communities in the long term. Sci. Adv. 6, eaay4054.

Reisser, J., Slat, B., Noble, K., du Plessis, K., Epp, M., Proietti, M., et al., 2014. The vertical distribution of buoyant plastics at sea. Biogeosci. Discuss. 11.

Rist, S., Vianello, A., Winding, M.H.S., Nielsen, T.G., Almeda, R., Torres, R.R., et al., 2020. Quantification of plankton-sized microplastics in a productive coastal Arctic marine ecosystem. Environ. Pollut. 266, 115248.

Rogers, K.L., Carreres-Calabuig, J.A., Gorokhova, E., Posth, N.R., 2020. Micro-by-micro interactions: how microorganisms influence the fate of marine microplastics. Limnol. Oceanogr. Lett. 5, 18–36.

Rüthi, J., Bölsterli, D., Pardi-Comensoli, L., Brunner, I., Frey, B., 2020. The "Plastisphere" of biodegradable plastics is characterized by specific microbial taxa of alpine and Arctic soils. Front. Environ. Sci. 8, 562263.

Schloss, P.D., Westcott, S.L., Ryabin, T., Hall, J.R., Hartmann, M., Hollister, E.B., et al., 2009. Introducing mothur: open-source, platform-independent, community-supported software for describing and comparing microbial communities. Appl. Environ. Microbiol. 75, 7537–7541.

Schwarz, A., Ligthart, T., Boukris, E., Van Harmelen, T., 2019. Sources, transport, and accumulation of different types of plastic litter in aquatic environments: a review study. Mar. Pollut. Bull. 143, 92–100.

Scotto, V., Alabiso, G., Marcenaro, G., 1986. An example of microbiologically influenced corrosion: the behaviour of stainless steels in natural seawater. Bioelectrochem. Bioenerg. 16, 347–355.

Shah, A.A., Hasan, F., Hameed, A., Ahmed, S., 2007. Isolation and characterization of poly (3-hydroxybutyrate-co-3-hydroxyvalerate) degrading bacteria and purification of PHBV depolymerase from newly isolated Bacillus sp. AF3. Int. Biodeterior. Biodegradation 60, 109–115.

da Silva, T.H., Câmara, P.E., Pinto, O.H.B., Carvalho-Silva, M., Oliveira, F.S., Convey, P., et al., 2021. Diversity of fungi present in permafrost in the South Shetland Islands, Maritime Antarctic. Microb. Ecol. 1–10.

Singh, P., Singh, S.M., 2012. Characterization of yeast and filamentous fungi isolated from cryoconite holes of Svalbard, Arctic. Polar Biol. 35, 575–583.

Sułowicz, S., Bondarczuk, K., Ignatiuk, D., Jania, J.A., Piotrowska-Seget, Z., 2020. Microbial communities from subglacial water of naled ice bodies in the forefield of Werenskioldbreen, Svalbard. Sci. Total Environ. 723, 138025.

Tahon, G., Willems, A., 2017. Isolation and characterization of aerobic anoxygenic phototrophs from exposed soils from the Sør Rondane Mountains, East Antarctica. Syst. Appl. Microbiol. 40, 357–369.

Tan, L., Li, L., Ashbolt, N., Wang, X., Cui, Y., Zhu, X., et al., 2018. Arctic antibiotic resistance gene contamination, a result of anthropogenic activities and natural origin. Sci. Total Environ. 621, 1176–1184.

Tashyreva, D., Elster, J., Billi, D., 2013. A novel staining protocol for multiparameter assessment of cell heterogeneity in Phormidium populations (cyanobacteria) employing fluorescent dyes. PLoS One 8, e55283.

Tekman, M.B., Wekerle, C., Lorenz, C., Primpke, S., Hasemann, C., Gerdts, G., et al., 2020. Tying up loose ends of microplastic pollution in the Arctic: distribution from the sea surface through the water column to deep-sea sediments at the HAUSGARTEN observatory. Environ. Sci. Technol. 54, 4079–4090.

Velan, M., SheebaVarma, S., Gnanambigai, P., Lakshmi, M.B., 2012. Biodegradation of toluene in the contaminated soil by Mycoplana sp. MVMB2. Int. J. 3.

Viršek, M.K., Lovšin, M.N., Koren, Š., Kržan, A., Peterlin, M., 2017. Microplastics as a vector for the transport of the bacterial fish pathogen species *Aeromonas salmonicida*. Mar. Pollut. Bull. 125, 301–309.

Walseng, B., Jensen, T., Dimante-Deimantovica, I., Christoffersen, K.S., Chertoprud, M., Chertoprud, E., et al., 2018. Freshwater diversity in Svalbard: providing baseline data for ecosystems in change. Polar Biol. 41, 1995–2005.

Wang, Q., Garrity, G.M., Tiedje, J.M., Cole, J.R., 2007. Naive Bayesian classifier for rapid assignment of rRNA sequences into the new bacterial taxonomy. Appl. Environ. Microbiol. 73, 5261–5267.

Wang, L., Deng, S., Wang, S., Su, H., 2017. Analysis of aerobic granules under the toxic effect of ampicillin in sequencing batch reactors: performance and microbial community. J. Environ. Manag. 204, 152–159.

Wang, J., Huang, M., Wang, Q., Sun, Y., Zhao, Y., Huang, Y., 2020a. LDPE microplastics significantly alter the temporal turnover of soil microbial communities. Sci. Total Environ. 726, 138682.

Wang, S., Xue, N., Li, W., Zhang, D., Pan, X., Luo, Y., 2020b. Selectively enrichment of antibiotics and ARGs by microplastics in river, estuary and marine waters. Sci. Total Environ. 708, 134594.

Webb, H.K., Crawford, R.J., Sawabe, T., Ivanova, E.P., 2008. Poly (ethylene terephthalate) polymer surfaces as a substrate for bacterial attachment and biofilm formation. Microbes Environ. 0812170036.

Woodall, L.C., Sanchez-Vidal, A., Canals, M., Paterson, G.L., Coppock, R., Sleight, V., et al., 2014. The deep sea is a major sink for microplastic debris. R. Soc. Open Sci. 1, 140317.

Wright, R.J., Langille, M.G., Walker, T.R., 2021. Food or just a free ride? A meta-analysis reveals the global diversity of the Plastisphere. ISME J. 15, 789–806.

Xiang, Q., Zhu, D., Chen, Q.-L., O'Connor, P., Yang, X.-R., Qiao, M., et al., 2019. Adsorbed sulfamethoxazole exacerbates the effects of polystyrene (~2 μm) on gut microbiota and the antibiotic resistome of a soil collembolan. Environ. Sci. Technol. 53, 12823–12834.

Yang, Y., Liu, G., Song, W., Ye, C., Lin, H., Li, Z., et al., 2019. Plastics in the marine environment are reservoirs for antibiotic and metal resistance genes. Environ. Int. 123, 79–86.

Yi, M., Zhou, S., Zhang, L., Ding, S., 2021. The effects of three different microplastics on enzyme activities and microbial communities in soil. Water Environ. Res. 93 (1), 24–32.

Zettler, E.R., Mincer, T.J., Amaral-Zettler, L.A., 2013. Life in the "plastisphere": microbial communities on plastic marine debris. Environ. Sci. Technol. 47, 7137–7146.

Zhang, T., Wang, N.-F., Zhang, Y.-Q., Liu, H.-Y., Yu, L.-Y., 2016. Diversity and distribution of aquatic fungal communities in the Ny-Ålesund region, Svalbard (high arctic). Microb. Ecol. 71, 543–554.

Zhang, M., Zhao, Y., Qin, X., Jia, W., Chai, L., Huang, M., et al., 2019. Microplastics from mulching film is a distinct habitat for bacteria in farmland soil. Sci. Total Environ. 688, 470–478.

Zhao, S., White, D.G., Ge, B., Ayers, S., Friedman, S., English, L., et al., 2001. Identification and characterization of integron-mediated antibiotic resistance among Shiga toxin producing *Escherichia coli* isolates. Appl. Environ. Microbiol. 67, 1558–1564.

Zhao, L., Su, C., Liu, W., Qin, R., Tang, L., Deng, X., et al., 2020. Exposure to polyamide 66 microplastic leads to effects performance and microbial community structure of aerobic granular sludge. Ecotoxicol. Environ. Saf. 190, 110070.

Zhao, Y., Gao, J., Wang, Z., Dai, H., Wang, Y., 2021. Responses of bacterial communities and resistance genes on microplastics to antibiotics and heavy metals in sewage environment. J. Hazard. Mater. 402, 123550.

Supplementary Information

Microbial colonizers of microplastics in an Arctic freshwater lake

Miguel González-Pleiter[1†], David Velázquez[1†], María Cristina Casero[2], Bjorn Tytgat[3], Elie Verleyen[4], Francisco Leganés[1], Roberto Rosal[4], Antonio Quesada[1] and Francisca Fernández-Piñas[1,*]

[1] Departamento de Biología, Universidad Autónoma de Madrid, Cantoblanco, E-28049 Madrid, Spain
[2] Departamento de Biogeoquímica y Ecología Microbiana, Museo Nacional de Ciencias Naturales, CSIC, E-28006 Madrid, Spain
[3] Laboratory of Protistology & Aquatic Ecology, Ghent University, Krijgslaan 281-S8, 9000 Gent, Belgium
[4] Department of Chemical Engineering, University of Alcalá, E-28871 Alcalá de Henares, Madrid, Spain

* Corresponding Author
† These authors contributed equally to this work
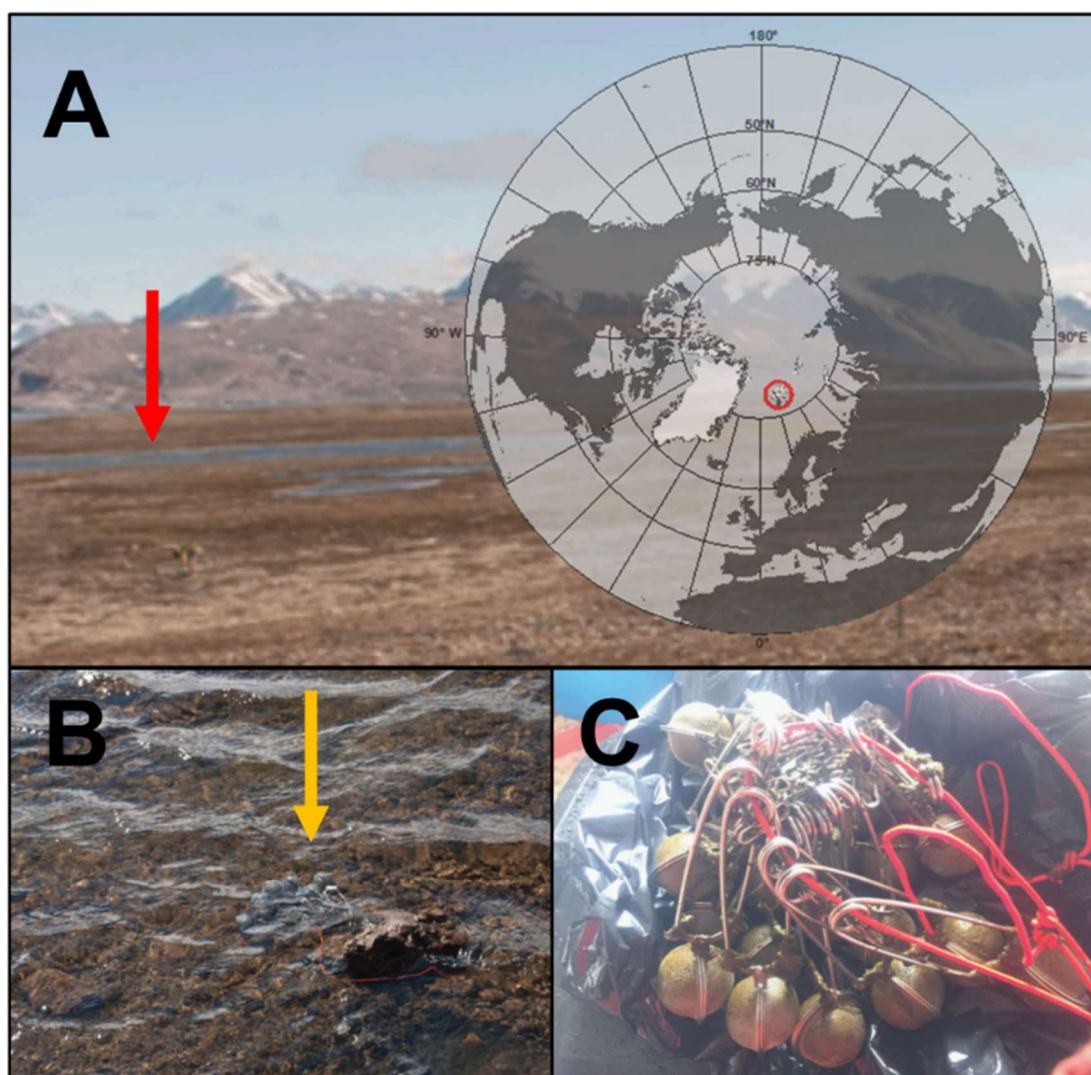
Figure S1. Location of the study area. A) General view of the study area. The red circle shows Svalbard Archipelago and red arrow indicates the Arctic freshwater lake where the experiment was carried out. B) Yellow arrow indicates the deployment of metallic cages with MPs into the Arctic freshwater lake. C) Metallic cages after eleven days of incubation into the lake.
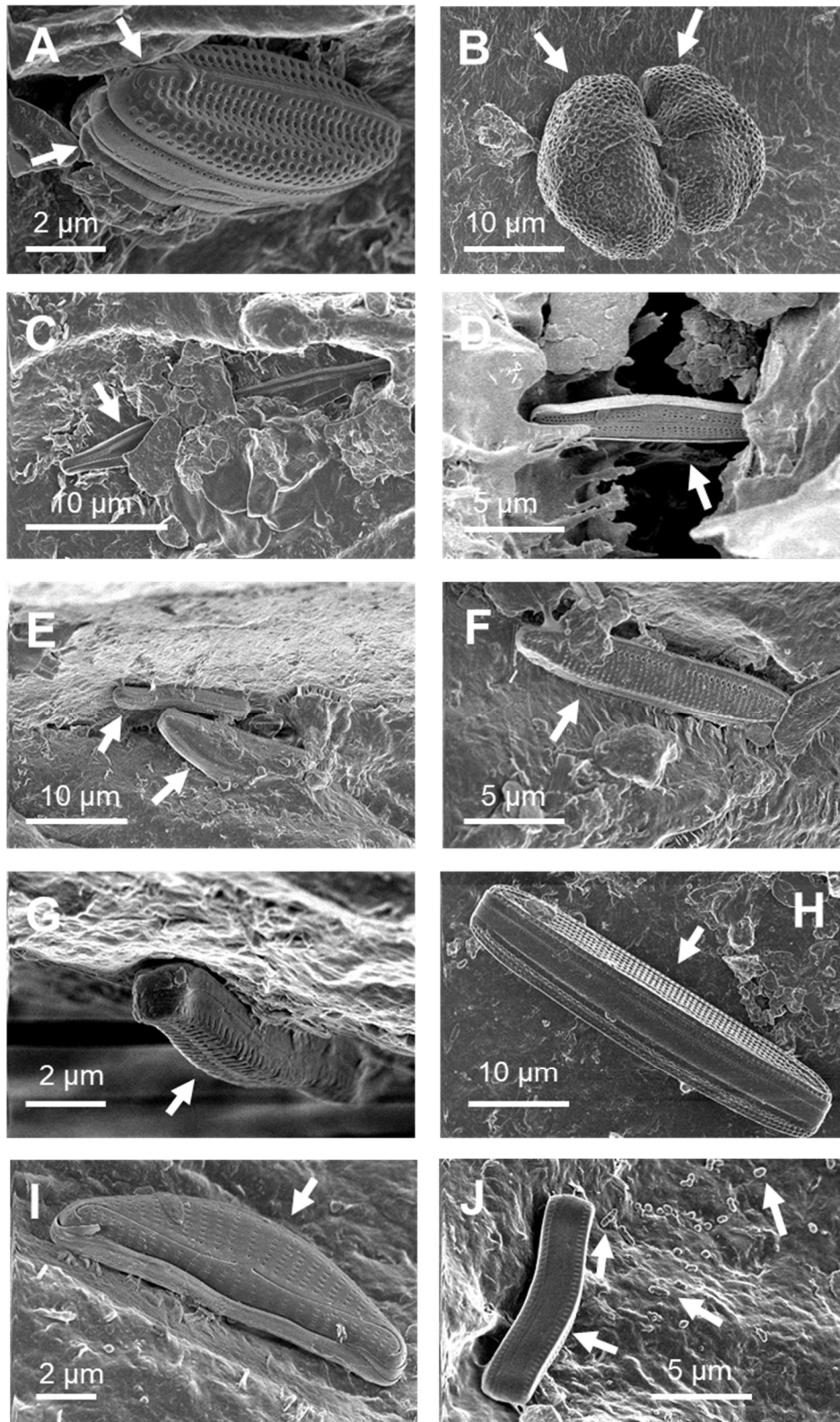
Figure S2. Scanning electron microscope (SEM) images of microbial colonizers on MPs incubated for eleven days in an Arctic freshwater lake: Arrows indicate: A) and B) dividing diatoms; C), D), E) and F) diatoms inside cavities; and G), H) and I) diatoms and J) bacteria and diatom attached to the surface.
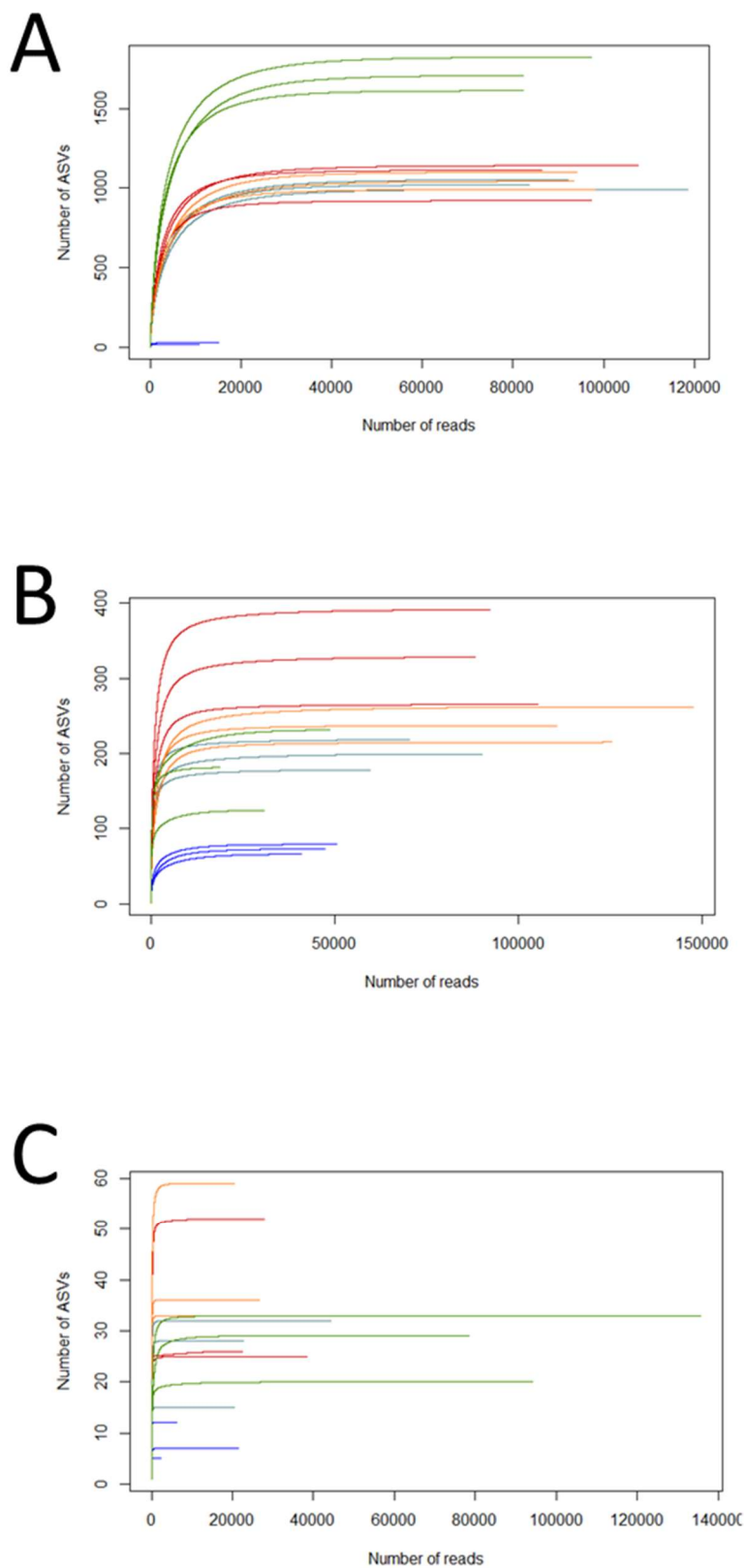
Figure S3. Rarefaction curve that compares the observed ASVs index of prokaryotes (A), eukaryotes (B) and fungi (C) in comparison with number of reads for each sample (sequencing depth).
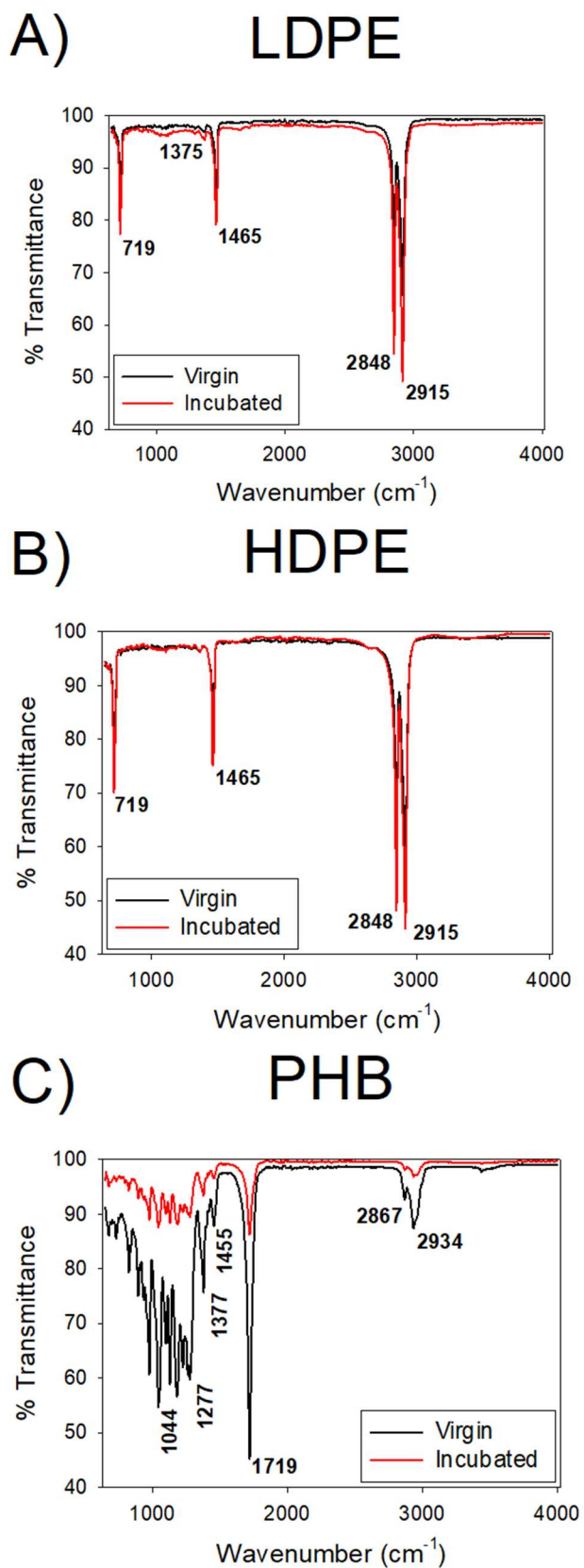
Figure S4. ATR-FTIR representative spectra of virgin and incubated MPs (LDPE -A-, HDPE -B- and PHB -C-).
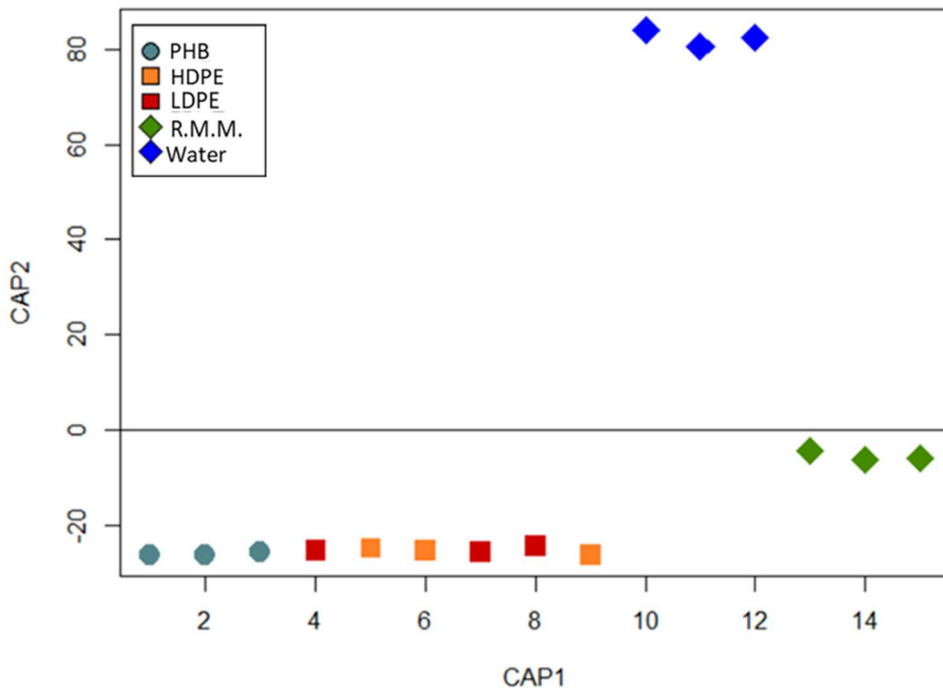
Figure S5. CAP analysis (canonical analysis of principal coordinates) of prokaryotic communities performed on Hellinger transformed based on ASV. Note: rock microbial mats (R.M.M.)
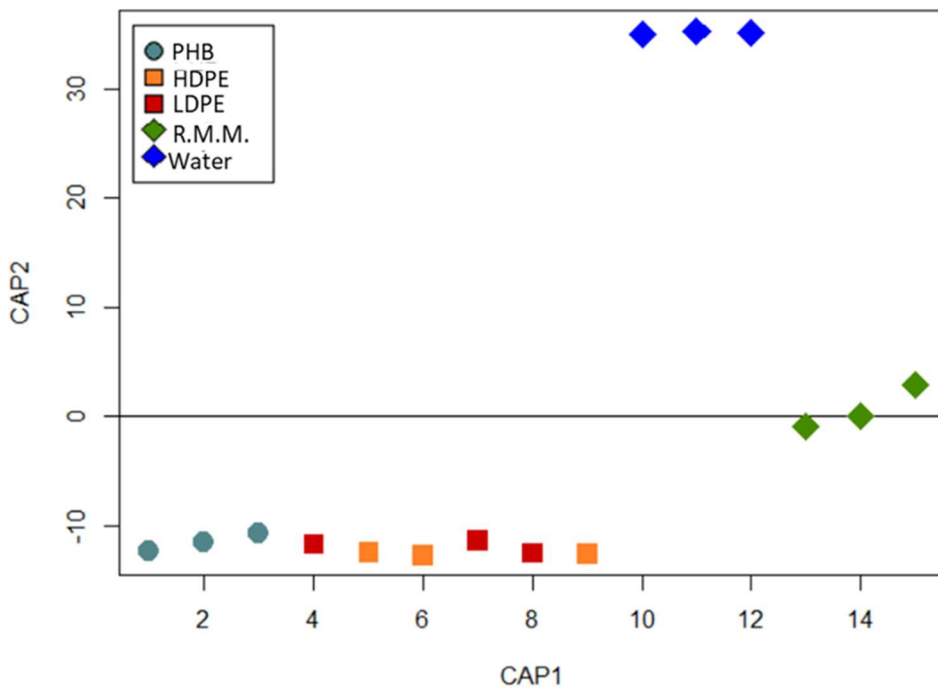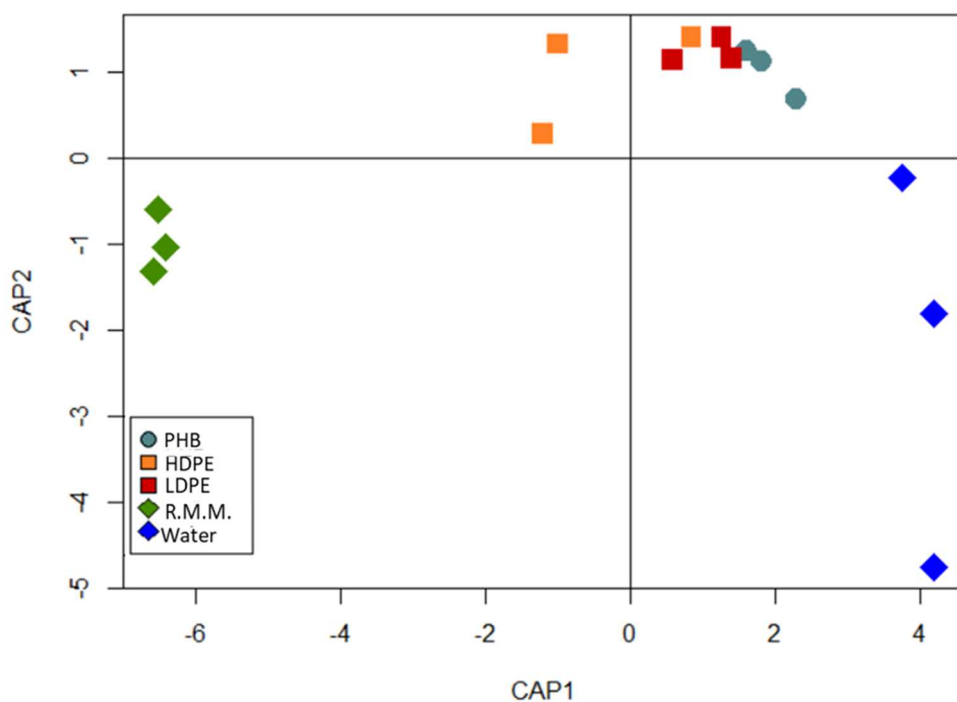

Figure S6. CAP analysis (canonical analysis of principal coordinates) of eukaryotic communities performed on Hellinger transformed based on ASV. Note: rock microbial mats (R.M.M.)

Figure S7. CAP analysis (canonical analysis of principal coordinates) of fungi communities performed on Hellinger transformed based on ASV.

Table S1. Primer pairs used in Illumina sequencing for 16S rRNA, 18S rRNA and ITS region.

Target gene/region	Primer	Sequence (5'–3')
16S rRNA	16SV3-V4-CS1	CCTACGGGNGGCWGCAG
	16SV3-V4-CS2	GACTACHVGGGTATCTAATCC
18S rRNA	18S-563f-CS1	GCCAGCAVCYGCGGTAAY
	18S-1132R-CS2	CCGTCAATTHCTTYAART
ITS	ITS4-CS1	TCCTCCGCTTATTGATATGC
	ITS86F-CS2	GTGAATCATCGAATCTTTGAA

Table S2. Primer pairs used in qPCR assays for detection and quantification of *sulI* and *ermB* antibiotic resistance genes.

Target gene	Primer	Sequence (5'–3')	Reference
16S rRNA	F1048	GTGSTGCAYGGYTGTCGTCA	Prio et al. 2016
	R1194	ACGTCRTCCMCACCTTCCTC	
sulI	sul(I)-FX	CGCACCGGAAACATCGCTGCAC	Prio et al. 2016
	sul(I)-RX	TGAAGTTCCGCCGCAAGGCTCG	
ermB	erm(B)-91f	GATACCGTTTACGAAATTGG	Prio et al. 2016
	erm(B)-454r	GAATCGAGACTTGAGTGTGC	

Reference

Proia, L., von Schiller, D., Sànchez-Melsió, A., Sabater, S., Borrego, C. M., Rodríguez-Mozaz, S., & Balcázar, J. L. (2016). Occurrence and persistence of antibiotic resistance genes in river biofilms after wastewater inputs in small rivers. Environmental Pollution, 210, 121-128.

Table S3. Surface properties of the materials.

	ΔG_{SWS} (mJ/m^2)*	Sdr (%)**	Sku***
PHB	-59.5 ± 2.5	3.1 ± 0.8	3.4 ± 0.3
LDPE	--76.0 ± 5.9	16.7 ± 8.4	3.6 ± 0.6
HDPE	-82.9 ± 2.3	2.1 ± 0.6	2.7 ± 0.4

* *ΔG_{SWS}* is the Gibbs free energy of interaction. The more negative, the more hydrophobic is the surface.

** **Sdr** is the developed interfacial area ratio defined as the percentage of additional area due to texture if compared to planar area (zero represents a flat surface).

*** **Sku**: kurtosis of roughness profile; Sku > 3: spiked distribution with numerous high peaks and low valleys; Sku < 3: means few peaks and low valleys.

Table S4. Pairwise PERMANOVA analysis of Bray-Curtis distances after Holm correction of the amplicons assayed. Natural: Water plus MicMat

		Pseudo-F	*p* value adjusted
Bacteria			
Global	Surface	11.30	0.001
Pairwise	PHB – LDPE	4.26	1
	PHB – PE	4.17	1
	PHB – Water	26.64	1
	PHB – MicMat	10.19	1
	LDPE – PE	1.53	1
	LDPE – Water	20.75	1
	LDPE – MicMat	7.93	1
	PE – Water	22.03	1
	PE – MicMat	7.93	1
	Water – MicMat	12.81	1
Global	Surface description	5.62	0.001
Pairwise	Biodegradable – Non-Biodegradable	4.24	0.026
	Biodegradable – Natural	4.39	0.026
	Non-Biodegradable – Natural	7.15	0.015
Global	Origin	16.15	0.001
Pairwise	Plastic – Water	23.04	0.009
	Plastic – MicMat	11.92	0.014
	Water – MicMat	12.81	0.100
Eukaryotes			
Global	Surface	9.55	0.001
Pairwise	PHB – LDPE	1.72	0.30
	PHB – PE	6.62	0.62
	PHB – Water	31.46	0.89
	PHB – MicMat	5.04	0.56
	LDPE – PE	3.32	0.45
	LDPE – Water	25.62	0.86
	LDPE – MicMat	4.69	0.54
	PE – Water	158.33	0.98
	PE – MicMat	7.37	0.65
	Water – MicMat	9.66	0.71
Global	Surface description	5.38	0.001
Pairwise	Biodegradable – Non-Biodegradable	3.05	0.061
	Biodegradable – Natural	4.00	0.040
	Non-Biodegradable – Natural	7.41	0.012
Global	Origin	13.11	0.001
Pairwise	Plastic – Water	22.19	0.012

	Plastic – MicMat	8.75	0.012
	Water – MicMat	9.66	0.100
Fungi			
Global	Surface	2.15	0.001
Pairwise	PHB – LDPE	1.07	0.3
	PHB – PE	2.13	0.1
	PHB – Water	1.39	0.2
	PHB – MicMat	3.58	0.1
	LDPE – PE	1.82	0.1
	LDPE – Water	1.56	0.1
	LDPE – MicMat	3.83	0.1
	PE – Water	1.77	0.1
	PE – MicMat	3.24	0.1
	Water – MicMat	1.97	0.1
Global	Surface description	1.92	0.005
Pairwise	Biodegradable – Non-Biodegradable	1.42	0.139
	Biodegradable – Natural	1.63	0.096
	Non-Biodegradable – Natural	2.41	0.012
Global	Origin	2.96	0.001
Pairwise	Plastic – Water	2.35	0.200
	Plastic – MicMat	4.40	0.009
	Water – MicMat	1.97	0.100

Table S5. Specific core microbiome identified at the genus-level resolution (prokaryotes, eukaryotes, and fungi) based on relative abundance ≥1 % for each type of tested substrates (Both non-biodegradable and biodegradable MPs, surrounding water and MicMat).

MPs						MicMat			Surrounding water		
Non-biodegradable (HDPE and LDPE)			Biodegradable (PHB)								
prokaryotes	eukaryotes	fungi	prokaryotes	eukaryotes	fungi	prokaryotes	eukaryotes	fungi	prokaryotes	eukaryotes	fungi
Mycoplana (25%)	**Ciliate**	*Betamyces* (17.6%)	*Mycoplana* (24.4%)	**Ciliate**	*Betamyces* (31.4%)	*Rhodobacter* (6.9%)	**Ciliate**	Ascomycota_ unclassified (49.2%)	*Polynucleobacter* (28.4%)	**Ciliate**	*Betamyces* (23.5%)
Erythromicrobium (7.6%)	*Stentor* (53.8%)	Chytridiomycota_ Unclassified (17.2%)	Moraxellaceae_ unclassified (8.1%)	*Stentor* (30.2%)	Chytridiomycota_ unclassified (25.3%)	*Gloeobacter* (6.4%)	*Stentor* (5.9%)	Helotiales_ unclassified (31.1%)	*Flavobacterium* (26.2%)	*Strombidiida_A_XX* (7.8%)	*Cladosporium* (20.2%) *Xylodon* (7.1%)
Rhodobacter (4.5%)	*Vorticella* (3.9%)	Chytridiomycota_ unclassified (4.9%)	*Rhodoferax* (6.0%)	*Vorticella* (14.6%)	Chytridiomycota_ unclassified (11.9%)	Acetobacteraceae_ unclassified (3.8%),	Ophryoglenida_unclassified (3.1%)	Chytridiomycota_ unclassified (8.7%)	*Limnohabitans* (14.2%)	Hypotrichia_ unclassified (1.8%)	Chytridiomycota_ unclassified (6.2%)
Comamonadaceae_ unclassified (4.0%)	*Uroleptus* (3.4%)	Didymellaceae_ unclassified (3.6%)	Comamonadaceae_ unclassified (5.8%)	Sessilida_unclassified (4.0%)	*Arrhenia* (3.6%)	Chitinophagaceae_ unclassified (3.6%),	Sessilida_unclassified (3.0%)	*Betamyces* (3.6%)	Cytophagaceae_ unclassified (12.9%)	**Algae**	Saccharomycetales_ unclassified (3.7%)
Sphingomonadaceae_unclassified (2.7%)	**Algae**	*Cryptococcus* (1.7%)	*Polaromonas* (4.0%)	*Uroleptus* (3.7%)	Polychytriales_ unclassified (1.3%)	*Leptolyngbya* (3.4%)	*Blepharisma* (1.1%)		Sphingomonadaceae_ unclassified (9.4%)	Chrysophyceae_Clade-C_ unclassified (82.1%)	Chytridiomycota_ unclassified (3.3%)
Zymomonas (2.5%)	*Epipyxis* (4.0%)	*Paranamyces* (1.5%)	Chilodonellidae_ unclassified (2.9%)	Chrysophyceae_Clade-C_ unclassified (4.8%)	*Malassezia* (1.0%)	Saprospiraceae_ unclassified (3.2%)	**Algae**		ACK-M1_ unclassified (2.8%)		*Cortinarius* (2.4%)
Pseudanabaena (2.2%)	Chrysophyceae_Clade-C_ unclassified (3.5%)	Helotiales_ Unclassified (1.2%)	*Erythromicrobium* (3.7%)	Chrysophyceae_CladeD_X (1.8%)		Bacteroidetes_ unclassified (3.1%)	*Phaeoplaca* (5.4%)		*Fluviicola* (1.6%)		Chytridiales_fam_Incertae_sedis_unclassified (1%)
Sphingomonas (2.1%)	*Cryptomonas* (3.0%)	*Xylodon* (1.0%)	*Rhodobacter* (3.2%)	*Chlamydomonas* (1.6%)		Alphaproteobacteria_ unclassified (2.6%)	Chrysophyceae_X_ unclassified (2.3%)		*Sediminibacterium* (1.5%)		
Novosphingobium (2.0%)	Chrysophyceae_X_ unclassified (2.2%)		*Zymomonas* (2.5%)	*Apocalathium* (1.4%)		*Pseudanabaena* (2.4%)	Chrysophyceae_Clade-D_X (1.5%)				
Caulobacter (1.8%)	*Tetraselmis* (1.9%)		*Flavobacterium* (2.3%)	**- Diatom**		Comamonadaceae_ unclassified (2.3%)	*Epipyxis* (1.0%)				
Synechococcus (1.6%)	Chrysophyceae_Clade-D_X (1.4%)		*Sphingomonas* (2.2%)	*Staurosira* (1.2%)		*Luteolibacter* (1.9%)	**- Diatom**				
Flavobacterium (1.5%)	*Chlamydomonas* (1.3%)		*Aquabacterium* (1.5%)			*Hyphomicrobium* (1.7%)	*Navicula* (9.9%)				
Rhodoferax (1.4%)			*Pseudanabaena* (1.4%)			*Leptothrix* (1.2%)	*Staurosira* (3.8%)				
Leptothrix (1.4%)			*Novosphingobium* (1.4%)			*Zymomonas* (1.1%)	*Cymbella* (2.1%)				
Polaromonas (1.2%)			*Paucibacter* (1.3%)			*Gemmata* (1.1%)	*Didymosphenia* (1.9%)				
Hydrogenophaga (1.2%)			*Caulobacter* (1.2%)			*Spirosoma* (1.0%)	*Achnanthidium* (1.0%)				
Luteolibacter (1.1%)			*Hydrogenophaga* (1.2%)			*Roseomonas* (1.0%)					
			Luteolibacter (1.2%)				**Other**				
			Leptothrix (1.1%)				*Rhizophydium* (2.7%)				